Lviv Polytechnic National University

Polymers in functionalization of nanoparticles and nanocomposites. Functional oligoperoxide-based luminescent and scintillation polymer and mineral nanocomposites. Applications in cellular research.

A. Zaichenko,
zaichenk@polynet.lviv.ua

Lviv Polytechnic National University

The aim of the study:

oligoperoxide based routes of tailored synthesis and functionalization of luminescent and scintillation polymer and mineral nanoparticles for biomedical application

Talk outline

I. Functional surface-active oligoperoxides and derived oligoelectrolyte and nonionic surfactants of block, comb-like or branched structures. Synthesis and characterization.

II. The main routes of the synthesis and functionalization of luminescent and scintillation polymeric and mineral nanoparticles

III. Cellular studies and potential biomedical application for pathological cell detection, tagging and treatment.

The main approaches of synthesis of functional oligoperoxide and derived polymeric surfactants

I. Functional reactive surface – active oligoperoxides and derived oligoelectrolytes and PEGylated oligomers of linear, block and comb-like structures.

The main approaches of synthesis of functional oligoperoxides and derived polymers

I.1. Copolymerization of unsaturated ditertiary peroxides with functional monomers.

I.2. Telomerisation of functional monomers in the presence of peroxide-containing telogen.

I.3. Polymer analogous transformations via reactions of carboxyl, amino, epoxy, isocyanate, anhydride and other reactive functional groups of peroxide-containing oligoelectrolytes.

I.1. Copolymerization of unsaturated ditertiary peroxides with functional monomers.

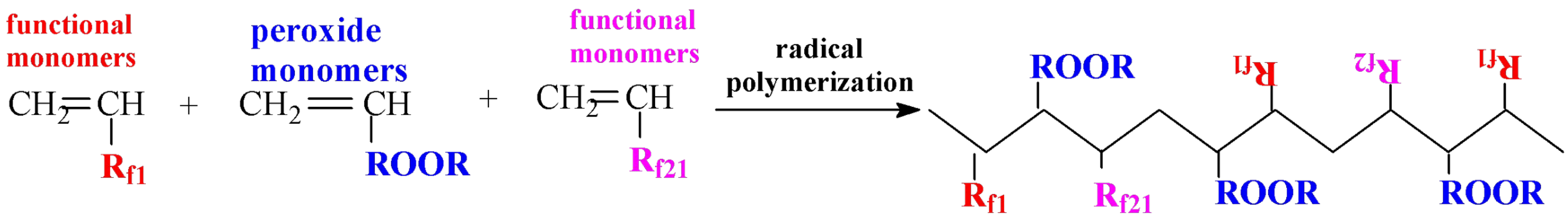

The general structure of surface - active linear oligoperoxides

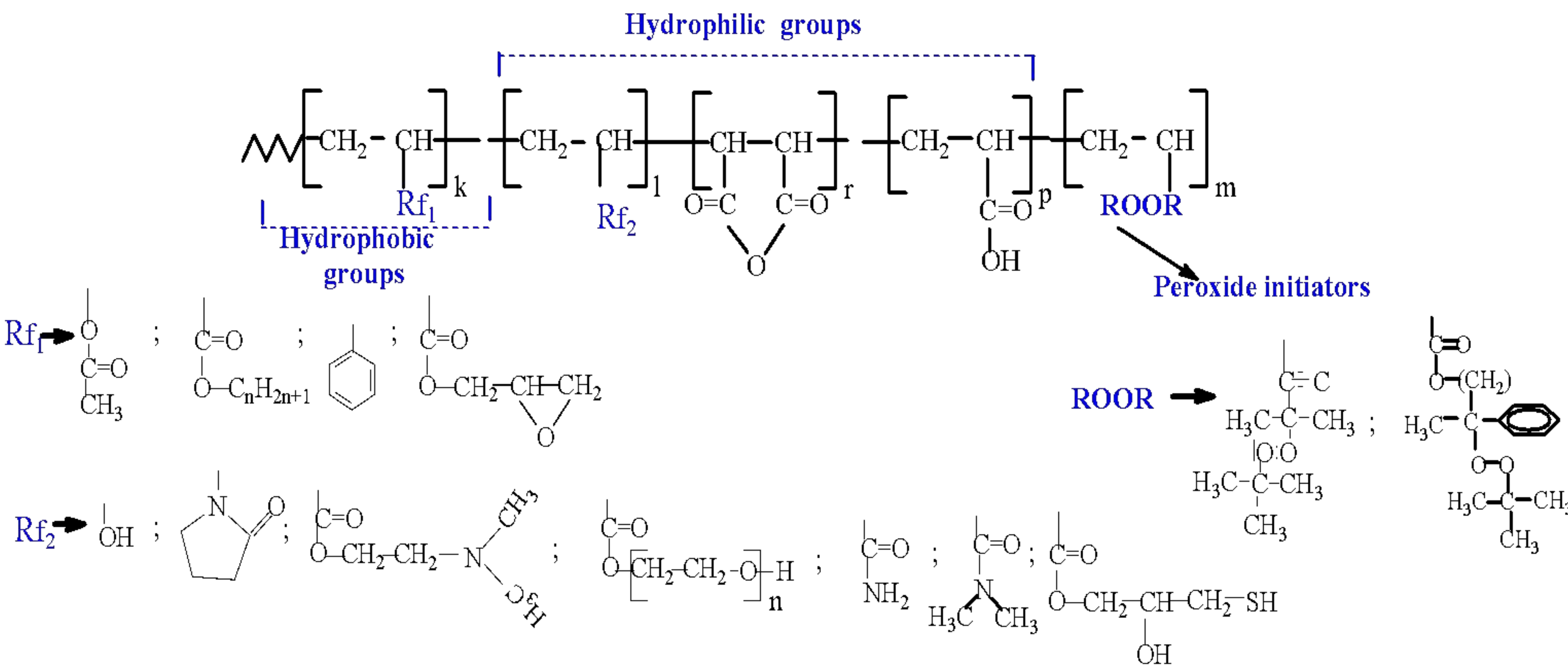

I.1. Oligoperoxide based synthesis of comb-like and branched oligo- and polyelectrolyte surfactants

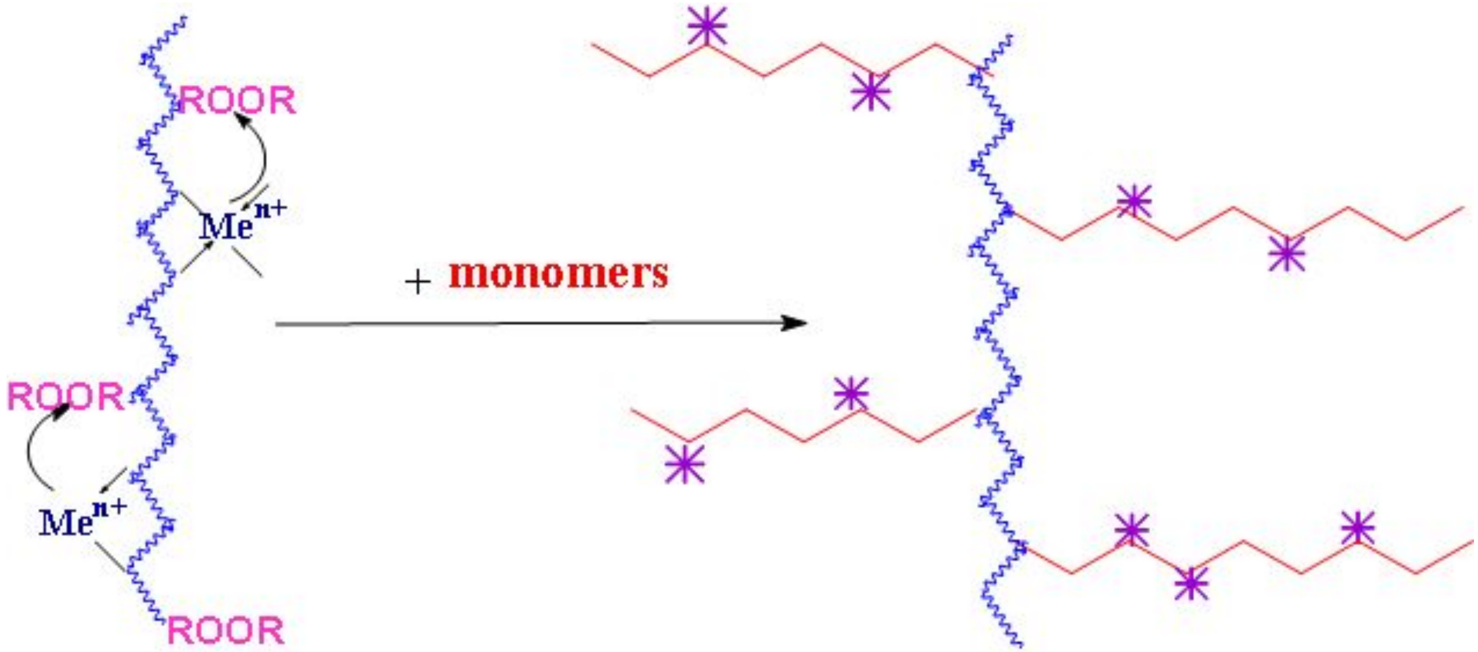

Oligoelectrolytes of comb-like and branched structures

I.1. Comb-like heterofunctional oligoelectrolyte surfactants

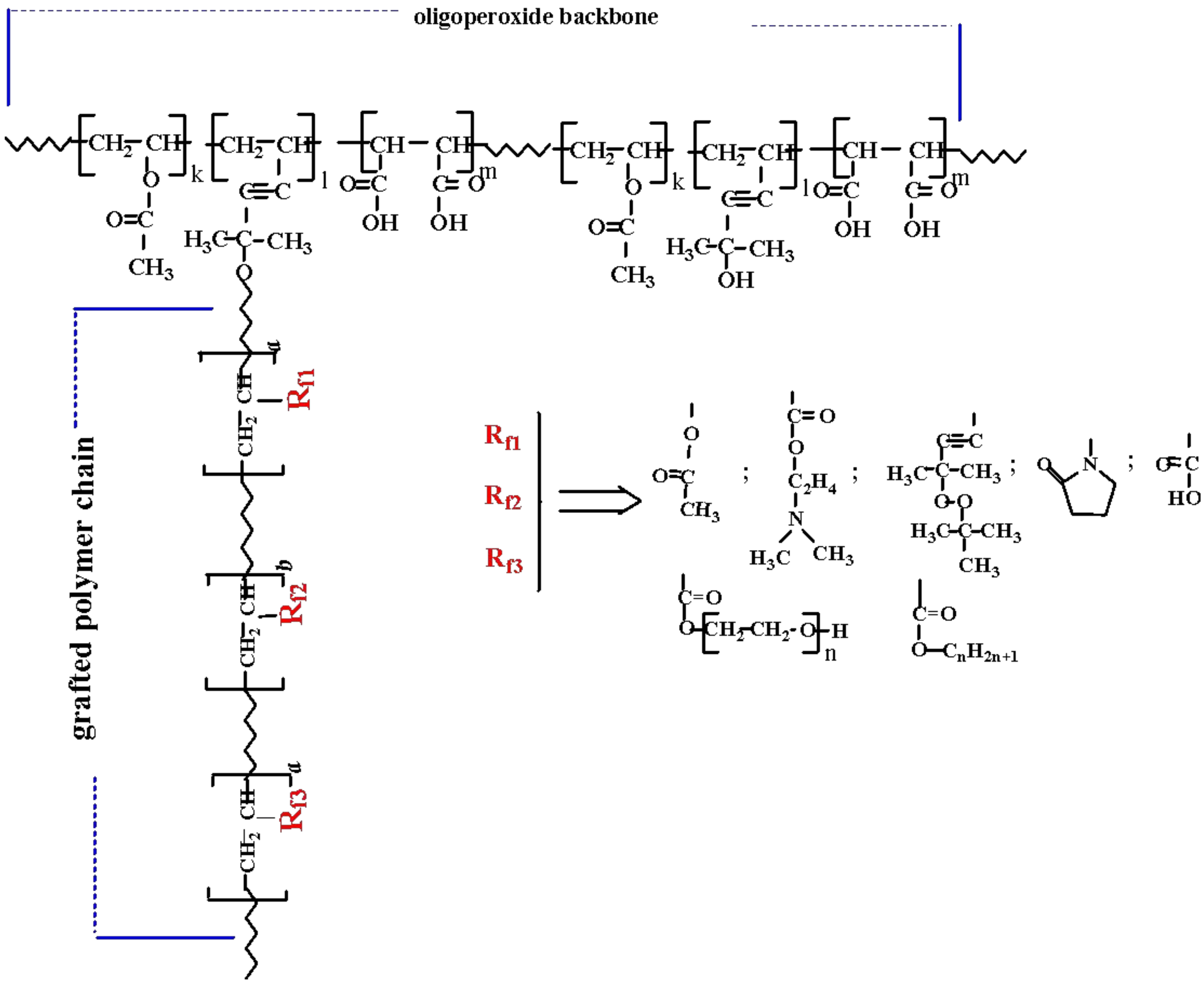

I.1. The general structure of cross-linked peroxide-containing oligoelectrolyte based microgels.

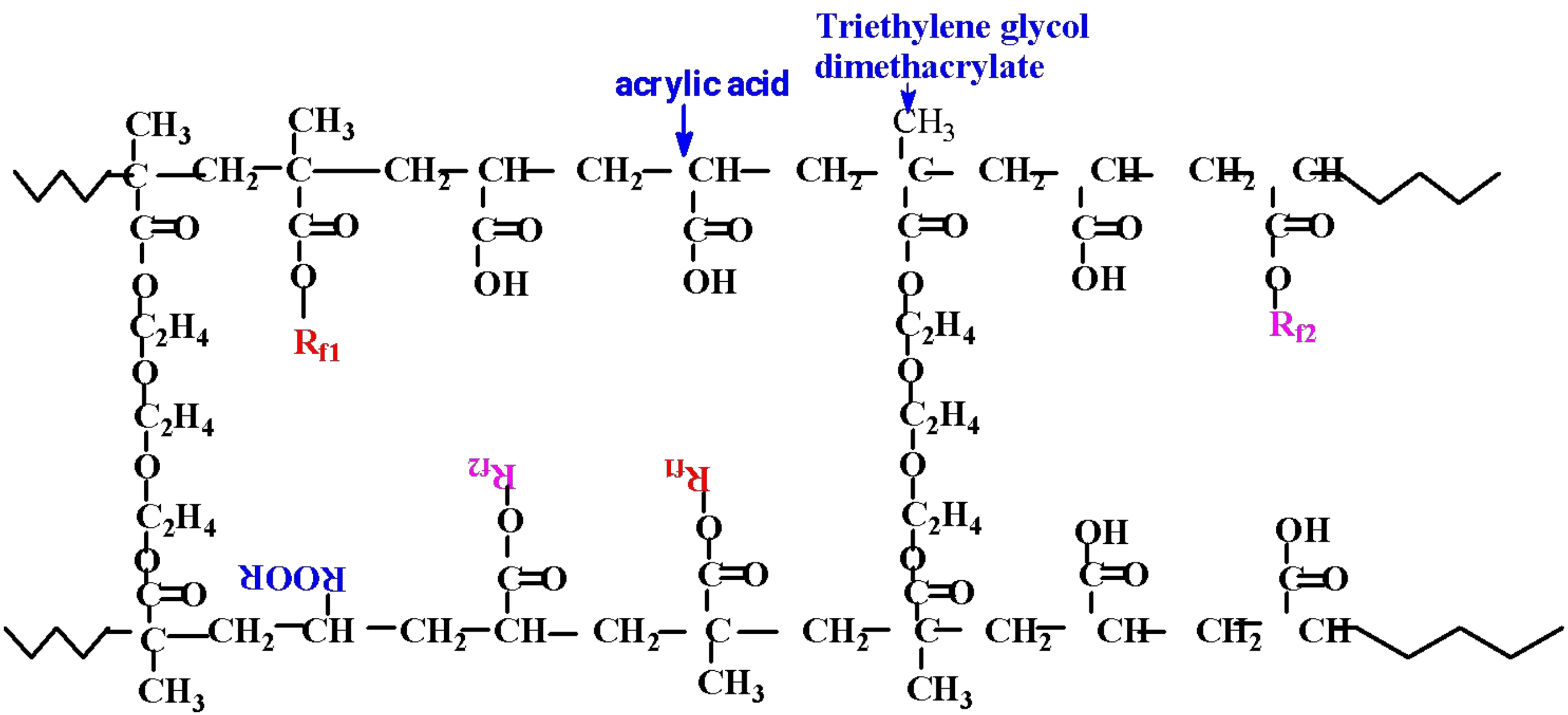

I.1. TEM images of oligoelectrolyte based nanogels

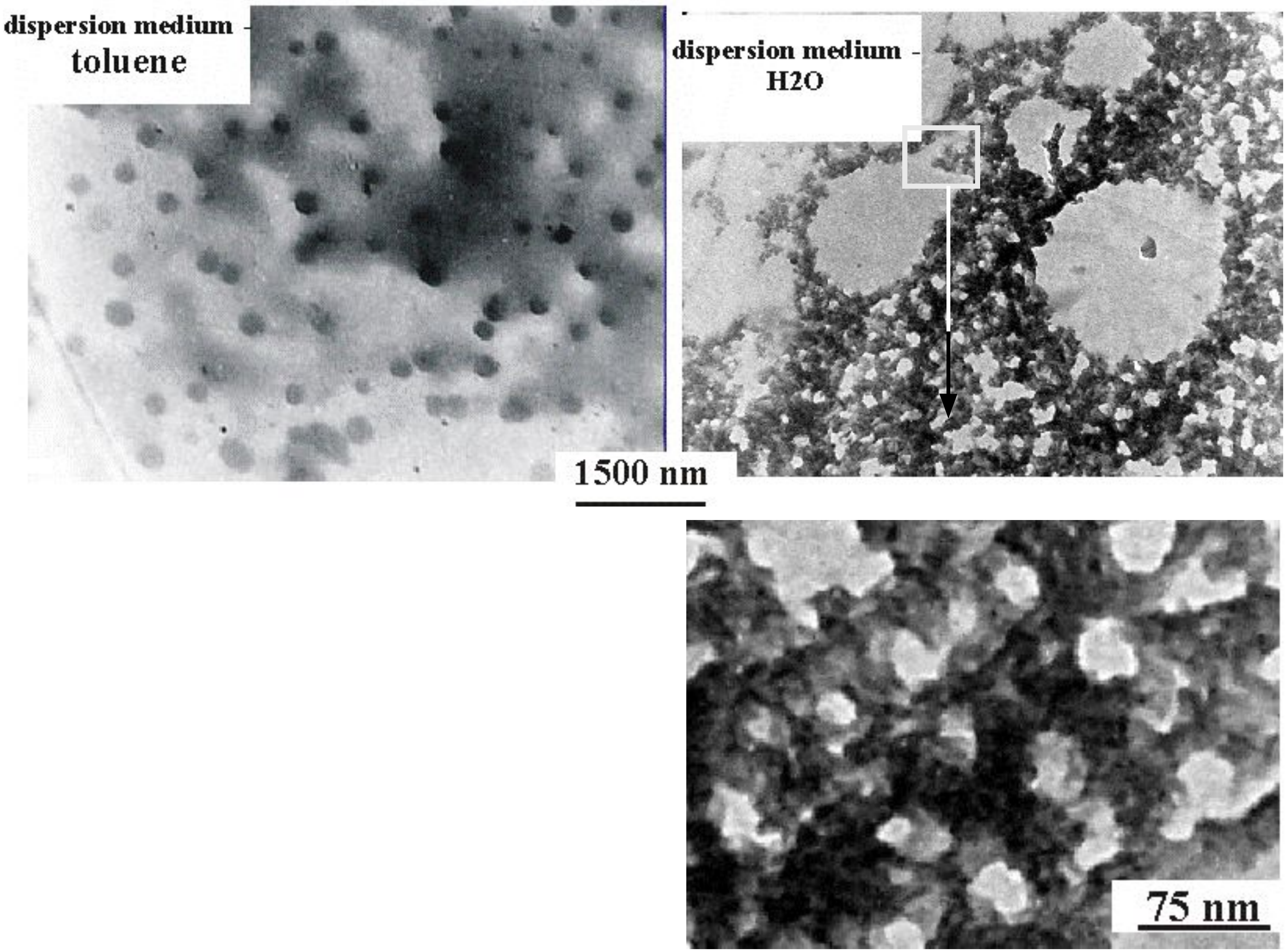

I.2. Surface-active oligoelectrolytes with end peroxide-containing fragment and derived block copolymers.

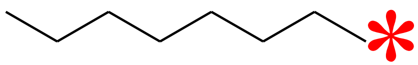

Oligoelectrolytes of telechelic structures

Oligoelectrolytes of block structures

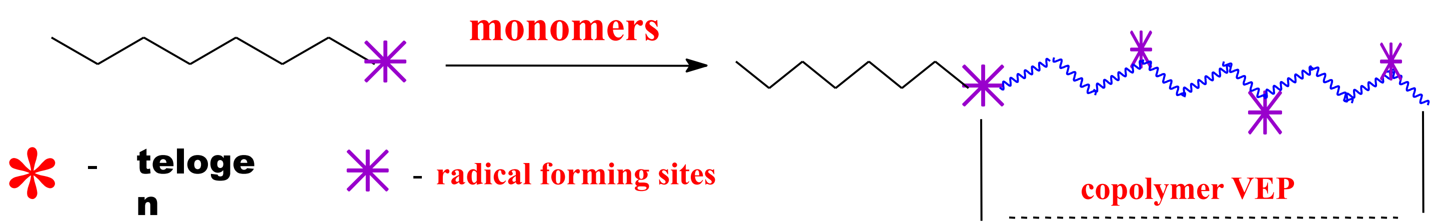

Chains comprising of vinyl alcohol, maleic acid, acrylic acid, DMAEMA and other links (M_N 1,500 – 6,000 g/mole).

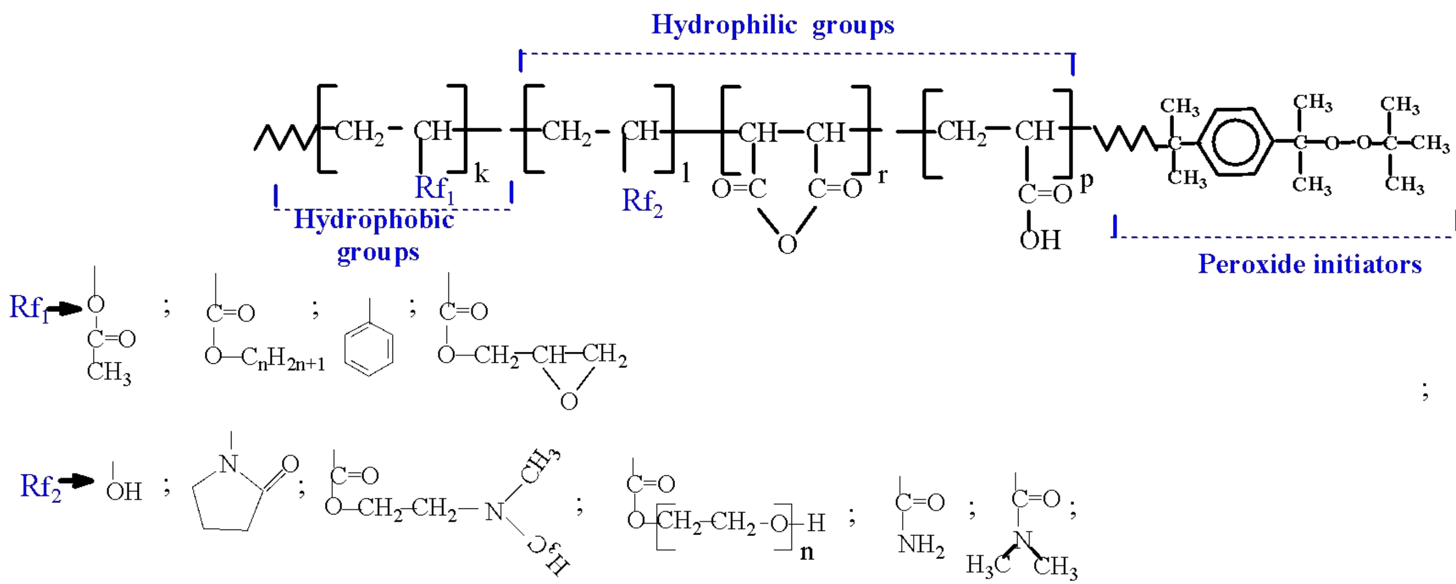

Telechelic oligoelectrolyte surfactants

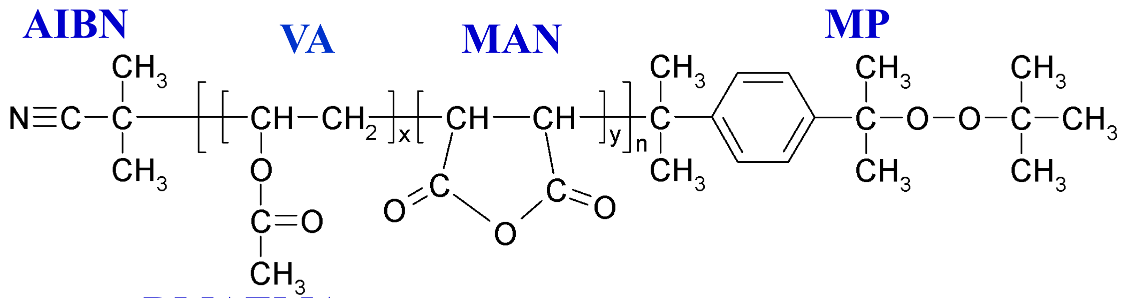

oligo(VA-MAN)-MP

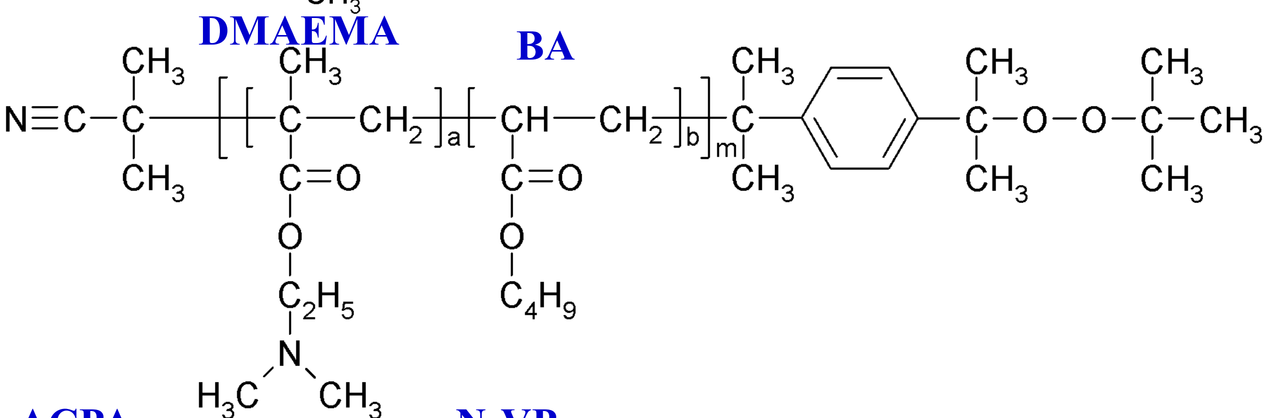

oligo(DMAEMA-BA)-MP

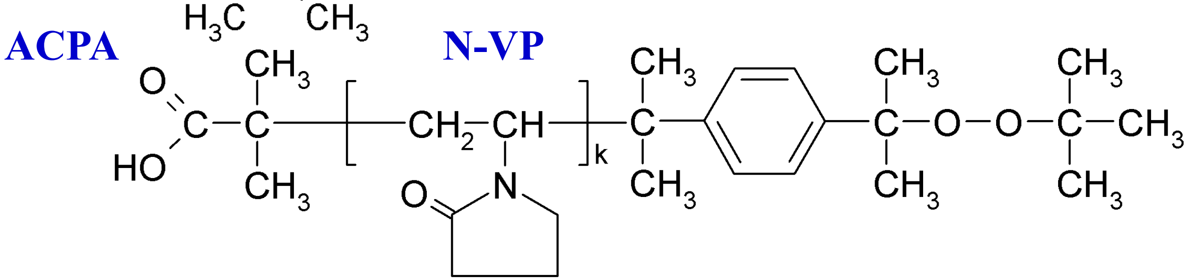

oligo(N-VP)-MP

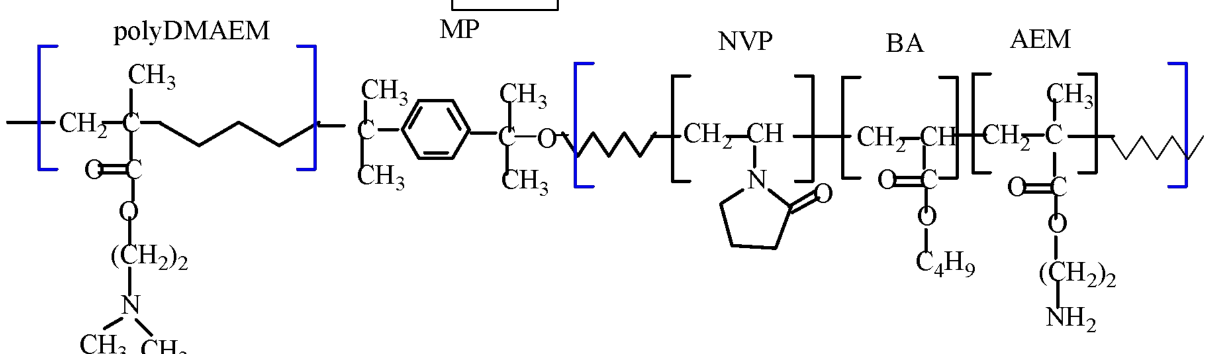

polyDMAEMA-block-copolyNVP-BA-AEM

I.3. Polymer analogous transformations via reactions of carboxyl, amino, epoxy, isocyanate, anhydride and other reactive functional groups of peroxide-containing oligoelectrolytes

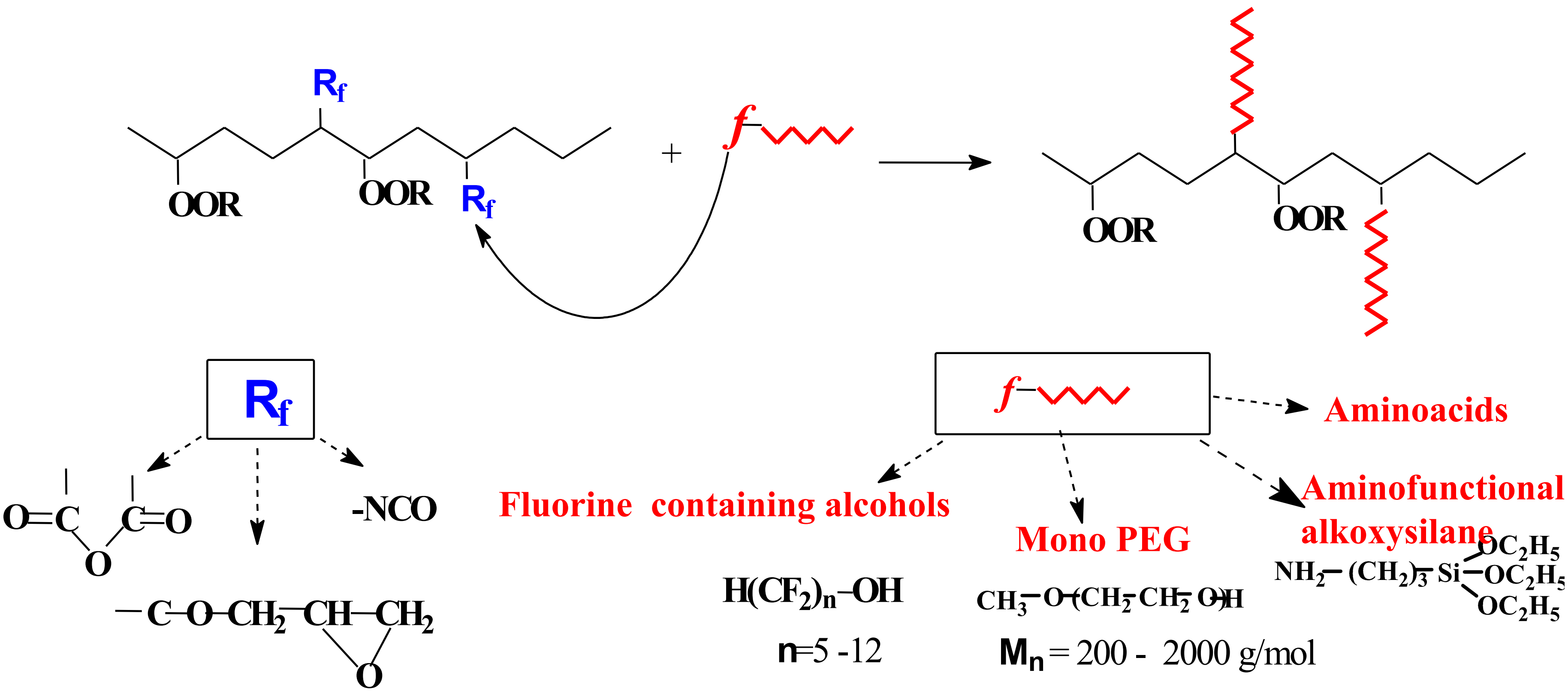

I.3. Polymer analogous transformations of peroxide-containing oligoelectrolytes via reactions of carboxyl, amino, epoxy, isocyanate, anhydride and other reactive functional groups

PEGylated oligoperoxides

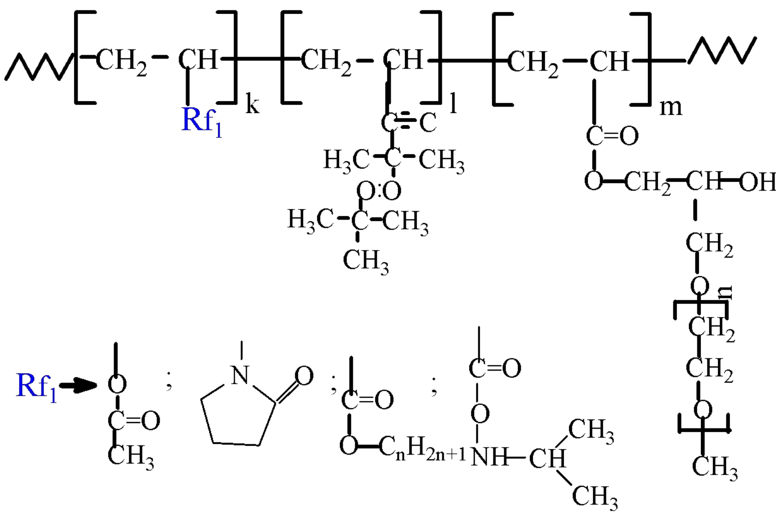

Polymeric surfactants combining PEG and polyelectrolute side chains

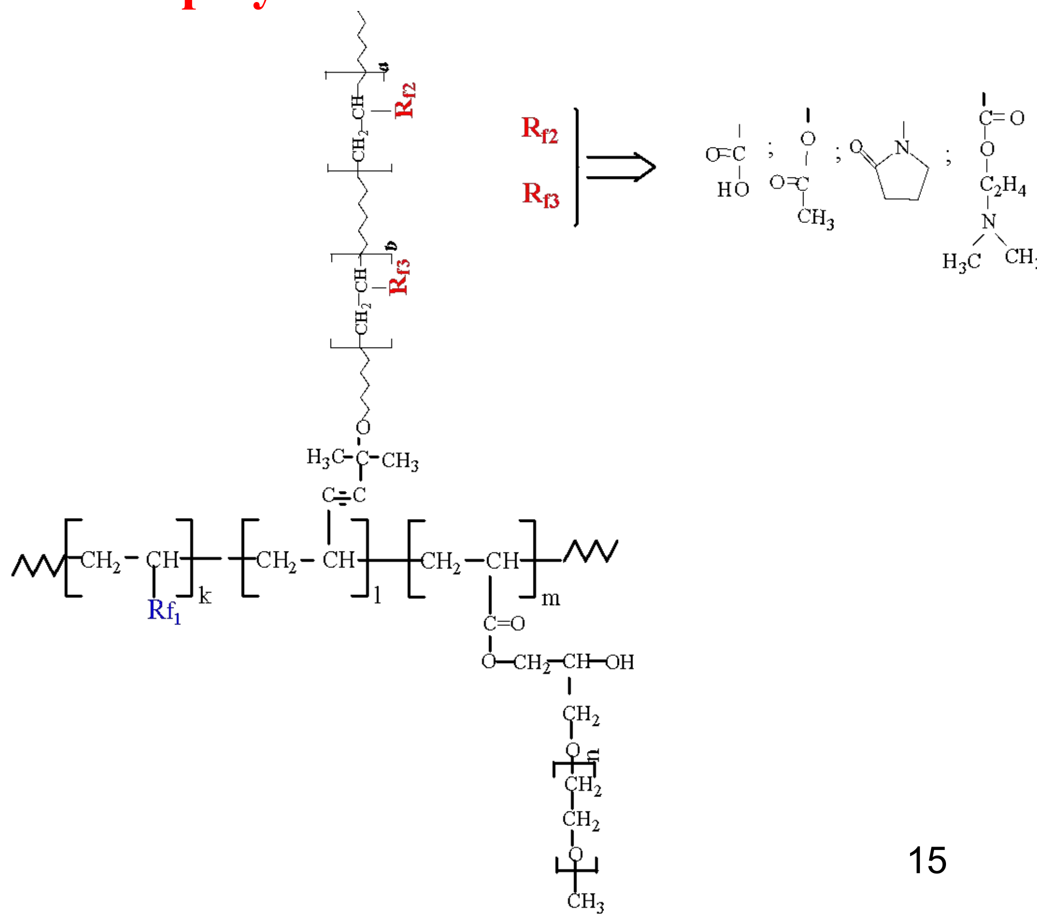

I.3. Polymeric salts and coordinating metal complexes of rare earth elements

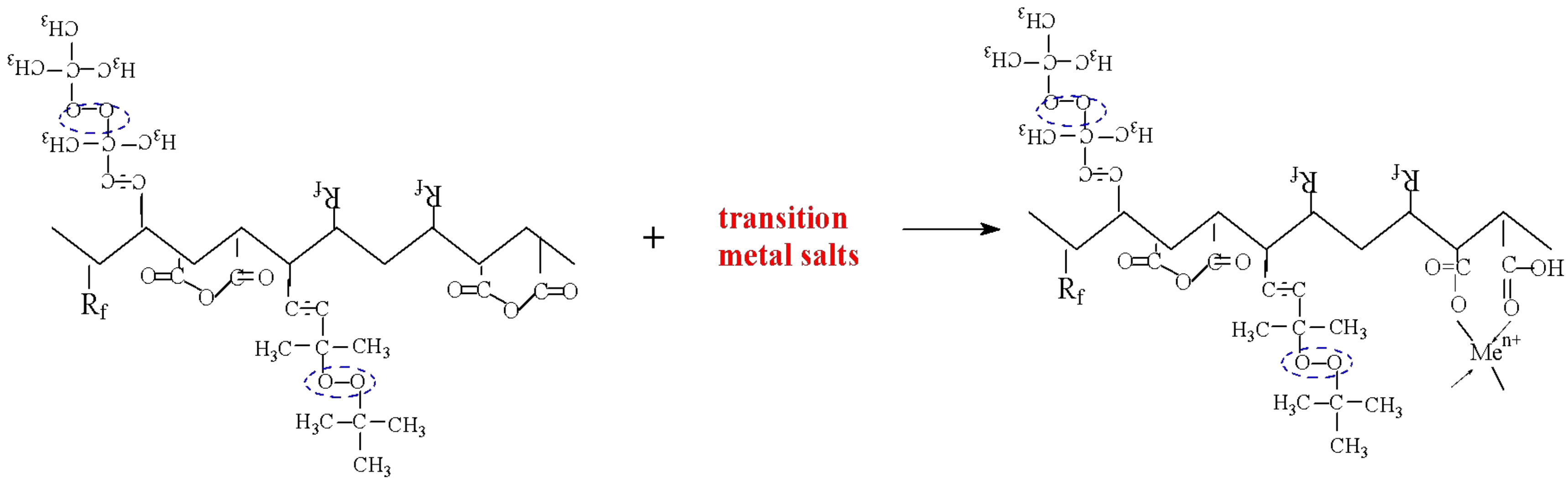

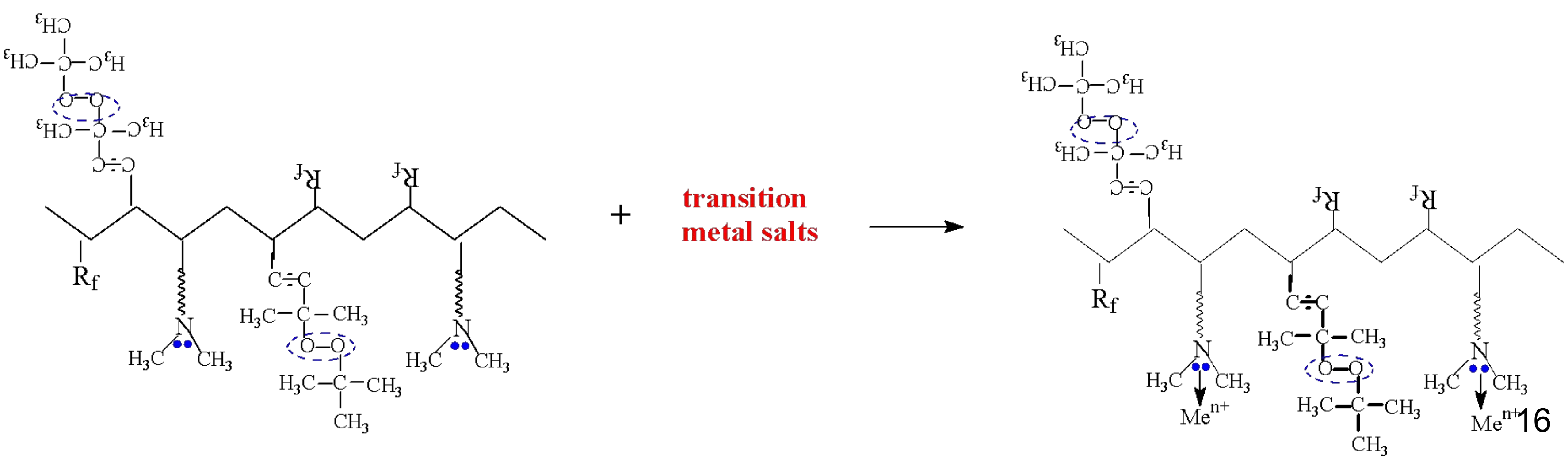

I. 3. Coordinating metal complexes of rare earth metal cations

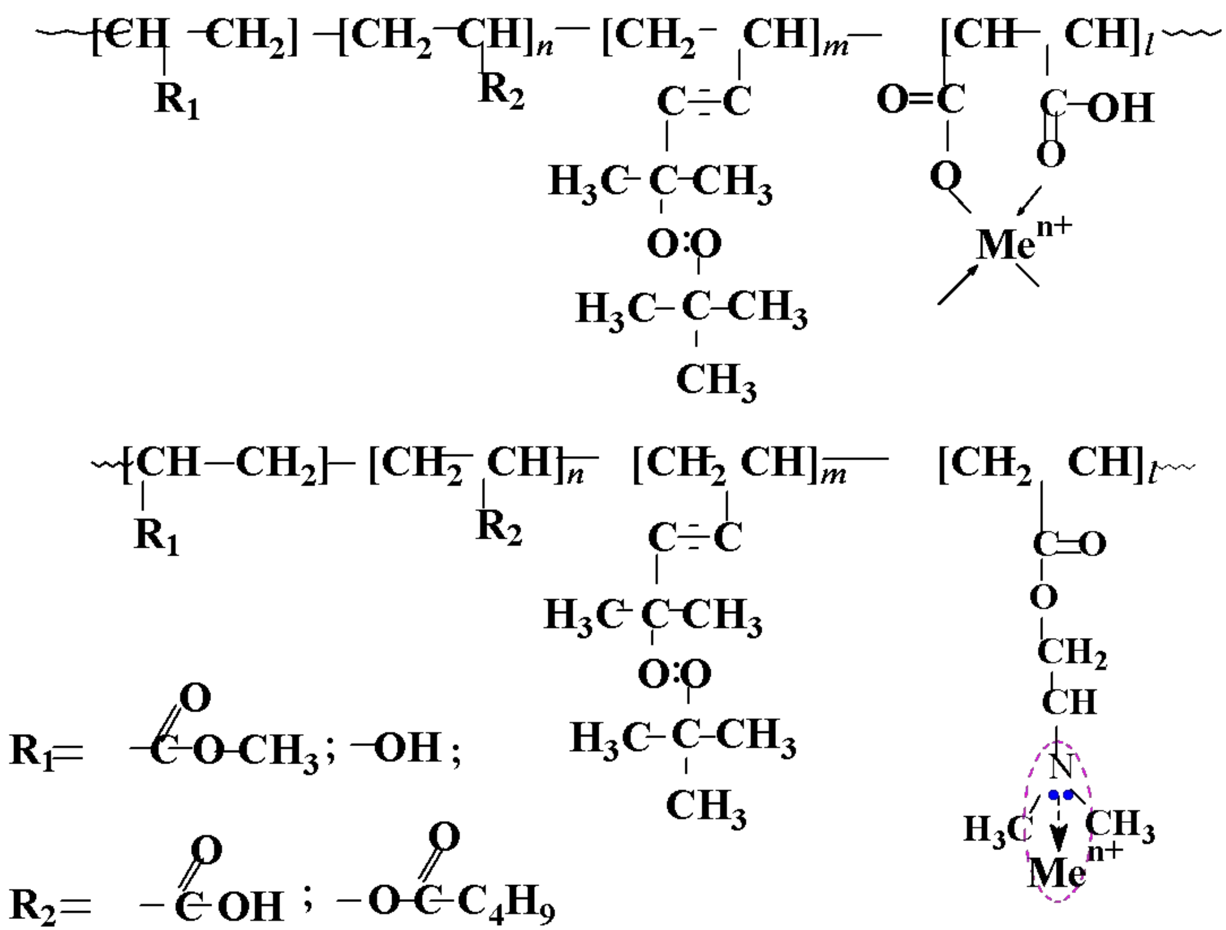

$Me^{n+} = Cu^{2+}, Co^{2+}, Ni^{2+}, Cr^{3+}, Eu^{3+}, Ce^{3+}$

Why these oligoperoxide based oligoelectrolytes?

- controlled design of a structure
- controlled molecular weight (1,000 – 30,000g/mole)
- narrowed molecular weight distribution
- controlled macro and microstructure
- controlled functionality and reactivity
- controlled solubility, surface activity
- biocompatibility and non toxicity
- Capability to form free radicals and initiate radical reactions

II. The main routes of the synthesis and functionalization of luminescent and scintillation polymeric and mineral nanoparticles

***Luminescent and scintillation properties of the materials were studied in I. Franko National University under the guidance of Professor A. Voloshinovskii**

II. The main routes of the synthesis and functionalization of luminescent and scintillation polymeric and mineral nanoparticles

II.1. Synthesis of polymeric salts and coordinating complexes of rare earth elements with oligoperoxide ligands (OMC) and luminescent polymeric nanoparticles (30 – 150nm) via water dispersion polymerization initiated and stabilized by OMC.

II.2. Synthesis of oligoperoxide and derived oligoelectrolyte surfactants containing luminescent fragments as a result of reactions with reactive phosphors.

II.3. Formation of nanosized micelle-like assemblies formed by oligoperoxide or oligoelectrolyte surfactants containing organic phosphors in hydrophobic core as a result of solubilization in water.

II.4. Synthesis of oligoelectrolyte based nanogels containing coordinated rare earth cations or filled with organic phosphors such as fluorescein in the pores.

II. The main routes of the synthesis and functionalization of luminescent and scintillation polymeric and mineral nanoparticles

II.5. Encapsulation of the phosphors (fluorescein, pyrazolyne and others) in the core of functional polymeric nanoparticles via water dispersion polymerization.

II.6. Template synthesis of functionalized mineral nanoparticles consisting of $LaPO_4$, $LuPO_4$, $LuBO_3$, GdF_3, CaF_2, BaF_2 salts doped with cations of Pr^{+3}, Ce^{+3}, Eu^{+2} and Eu^{+3} core and oligoperoxide shell possessing controlled luminescent and scintillation abilities and capable of grafting functional polymer chains.

II.7. Formation of luminescent nanolayers of controlled thickness and functionality on flat plate surfaces via deposition of functional polymeric and polymer-mineral nanocomposites and futher radical grafting functional polymeric brushes.

II.1. Coordinating complexes of rare earth elements with oligoperoxide ligands (OMC) and polymeric nanoparticles synthesized via water dispersion polymerization initiated by OMC.

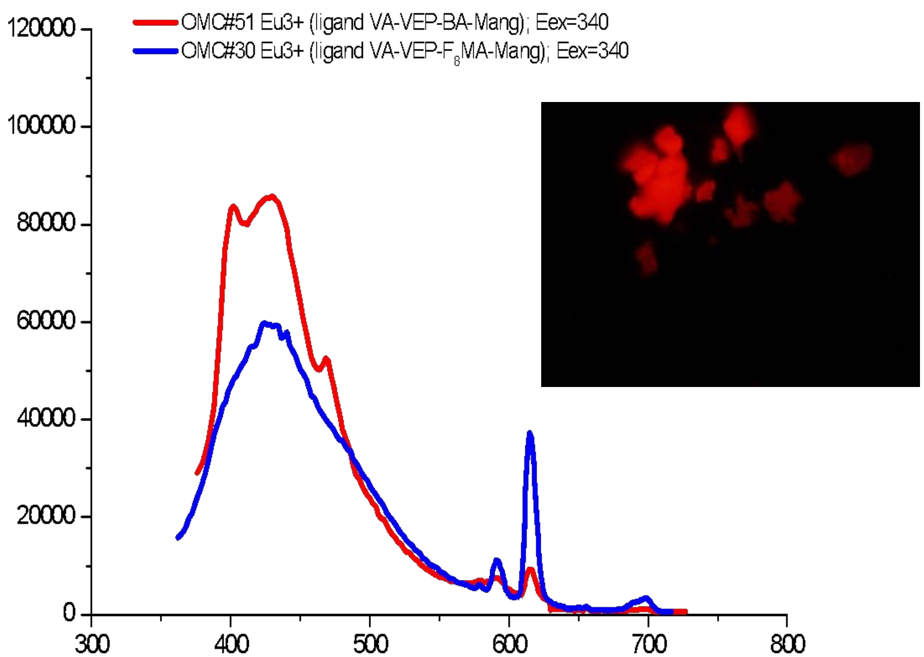

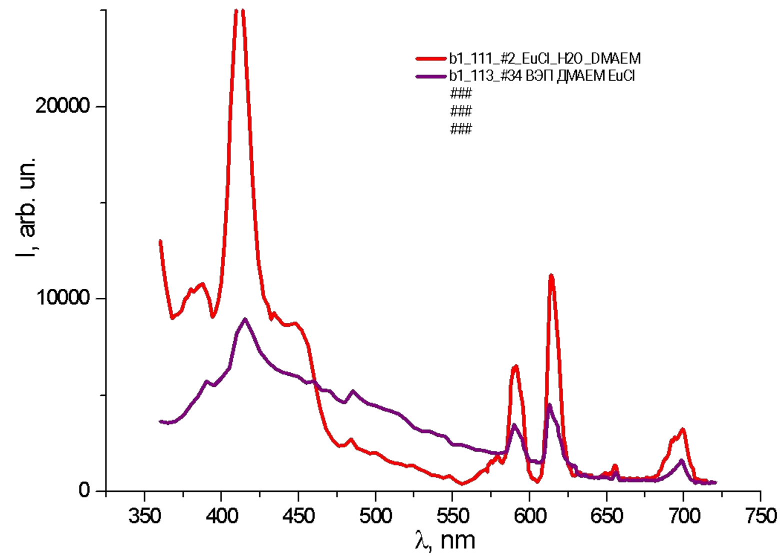

Spectra of luminescence of oligoperoxide metal complexes with Eu^{3+} on the basis copolymer of vinyl acetate (VA), VEP, maleic anhydride (MA) (1) and VA, VEP, MA and fluoro acrylate (2)

Spectra of luminescence of Eu^{3+} salt of oligoperoxide acrylonitrile (AN), VEP, dimethylaminoethyl methacrylate (DMAEM) (1) and VA, VEP DMAEM (2)

II.1. Coordinating complexes of rare earth elements with oligoperoxide ligands (OMC) and polymeric nanoparticles synthesized via water dispersion polymerization initiated by OMC.

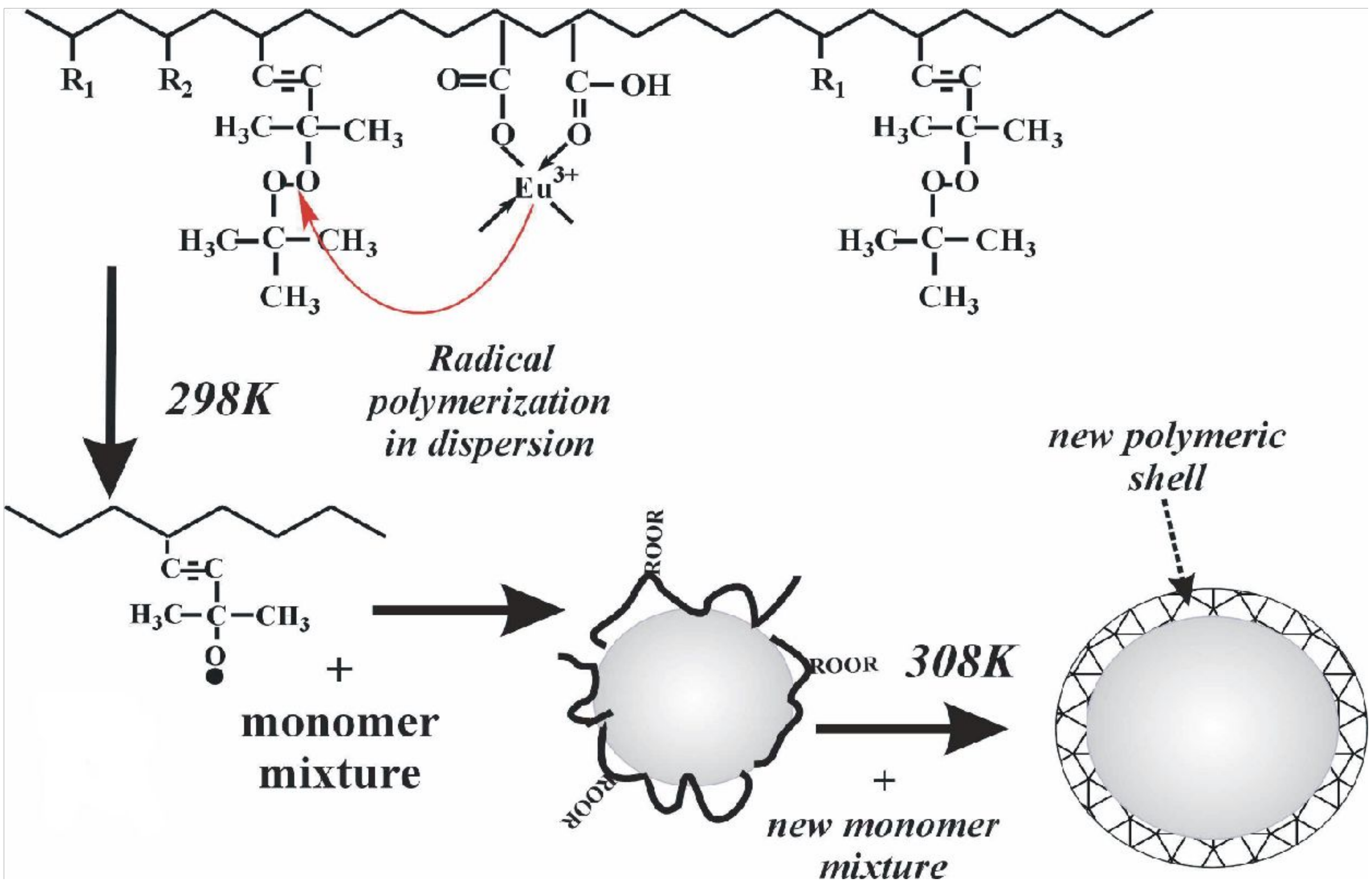

The scheme of the synthesis and functionalization of luminescent polymer NPs

II.1. Coordinating complexes of rare earth elements with oligoperoxide ligands (OMC) and polymeric nanoparticles synthesized via water dispersion polymerization initiated by OMC.

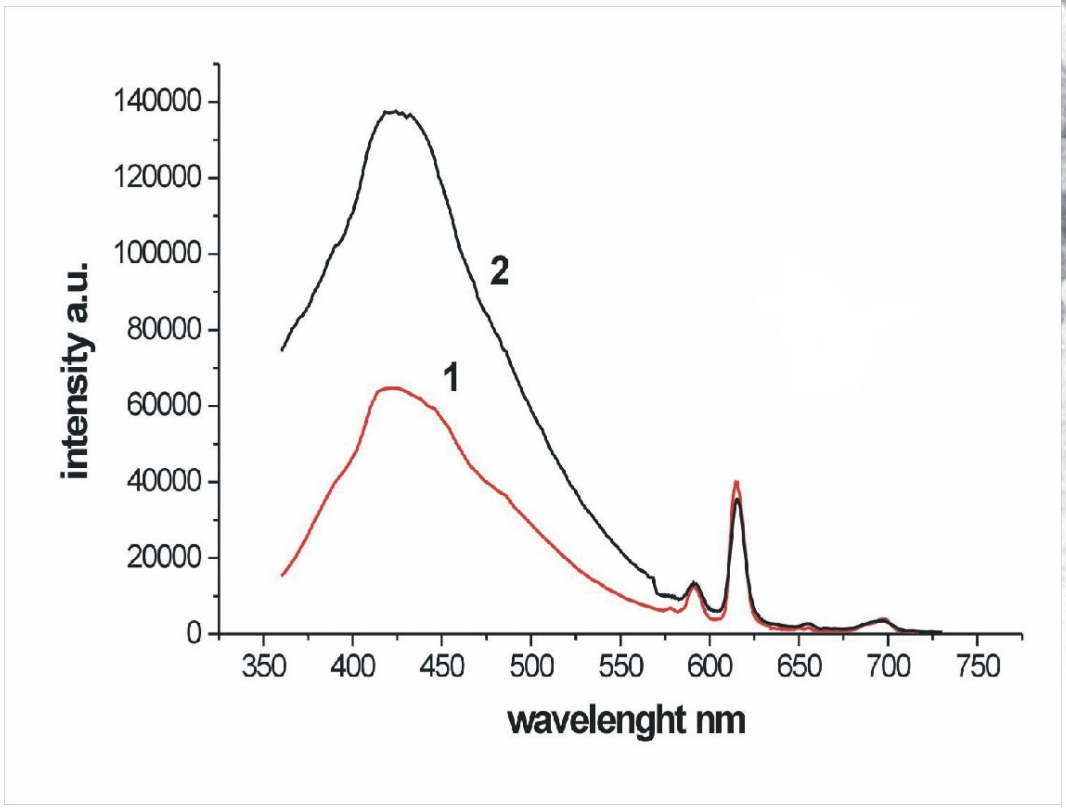

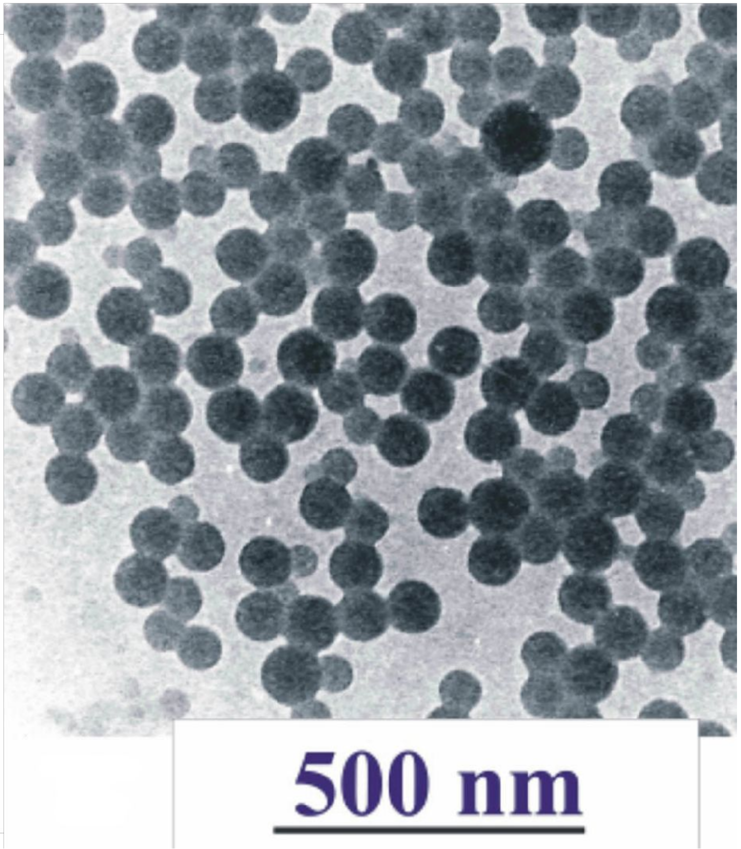

Luminescence spectrum (b) of Eu^{+3} containing OMC (1) and polymer NPs (2) synthesized in the presence of OMC; TEM images of luminescent NPs (c).

II.1. Coordinating complexes of rare earth elements with oligoperoxide ligands (OMC) and polymeric nanoparticles synthesized via water dispersion polymerization initiated by OMC.

The scheme of formation of functional polymer-mineral nanoparticles consisting of cured SiO2 core and oligoperoxide shell

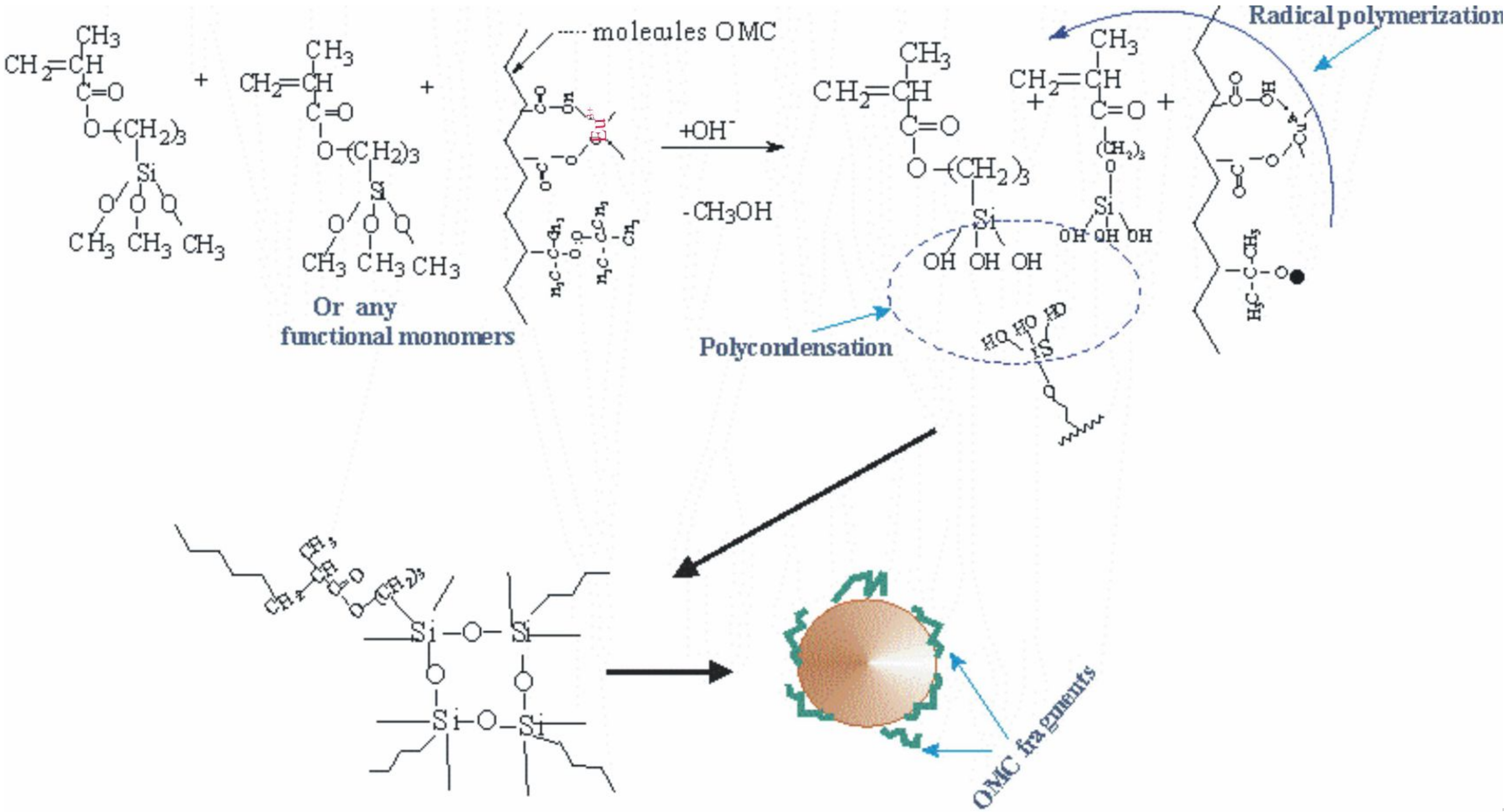

II.1. Coordinating complexes of rare earth elements with oligoperoxide ligands (OMC) and polymeric nanoparticles synthesized via water dispersion polymerization initiated by OMC.

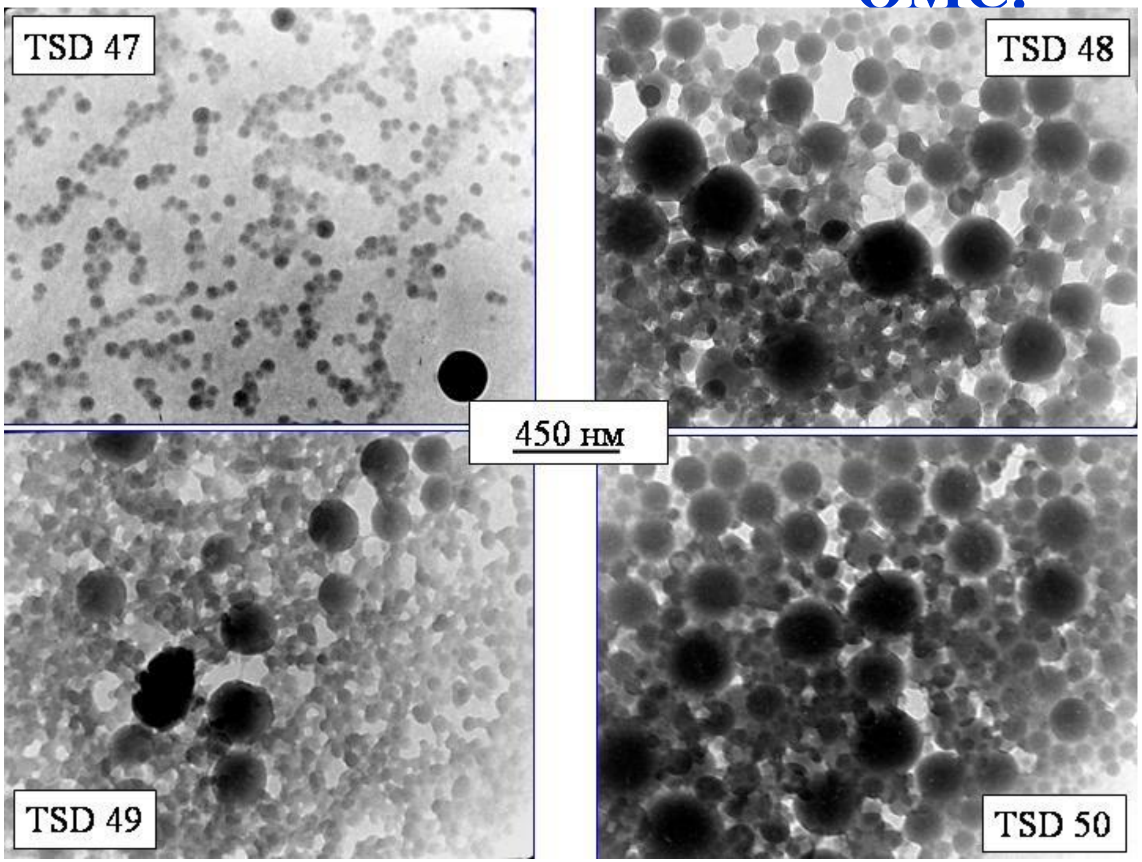

1H-29Si CP/MAS NMR at 4 kHz MAS

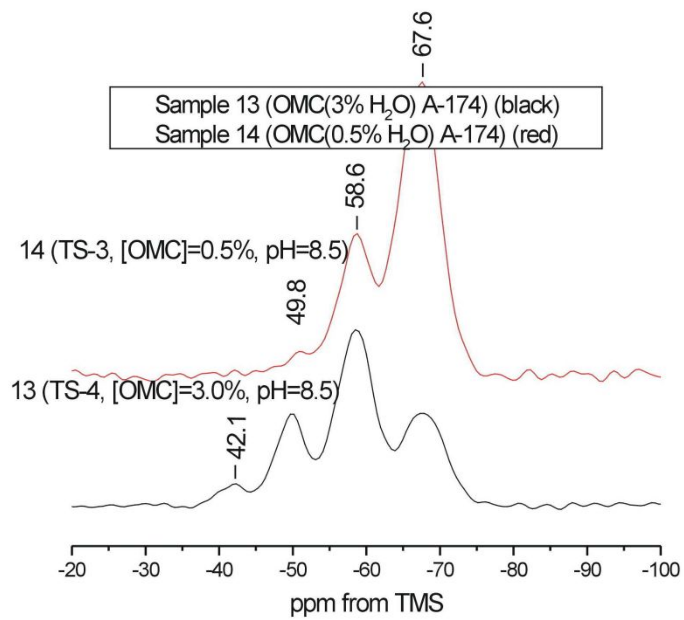

TEM изображения частиц поли Водные дисперсии поли-(Trimethoxysilyl)propyl methacrylate, полученные при инициировании ОМК, **$[OMC]_{in\ H2O}$=3% (TSD47; TSD48) и 0,5% (TSD47; TSD48); pH=8.5 (TSD47; TSD49) и 12 (TSD48; TSD50)** (298K, H_2O: Trimethoxysilyl)propyl methacrylate =7:1)

OMC=3% H2O (black) OMC=0.5% H2O (red)

II.2. Synthesis of oligoperoxide and derived oligoelectrolyte surfactants containing luminescent organic fragments.

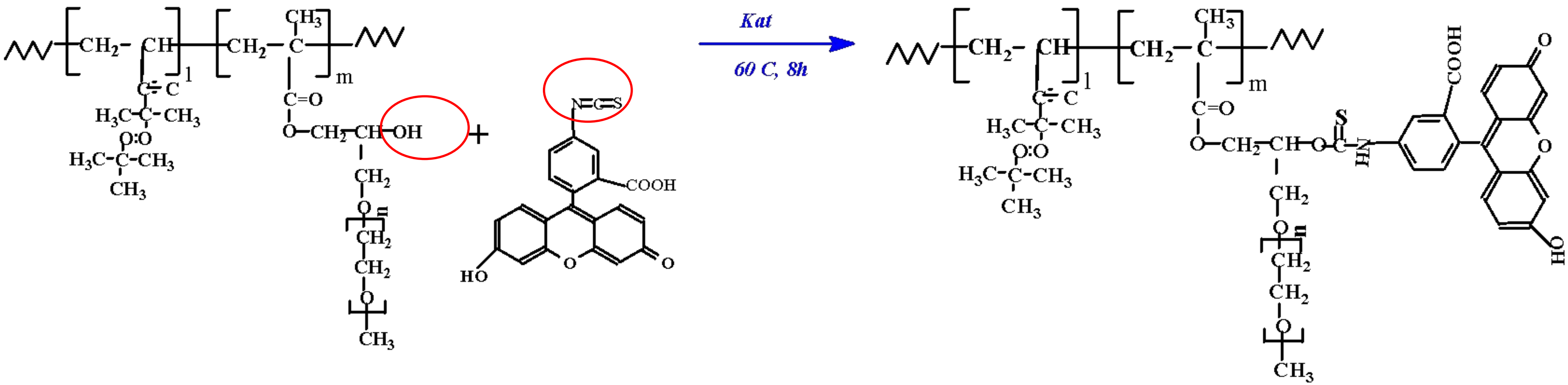

II.2. Synthesis of oligoperoxide and oligoelectrolyte surfactants containing luminescent organic fragments.

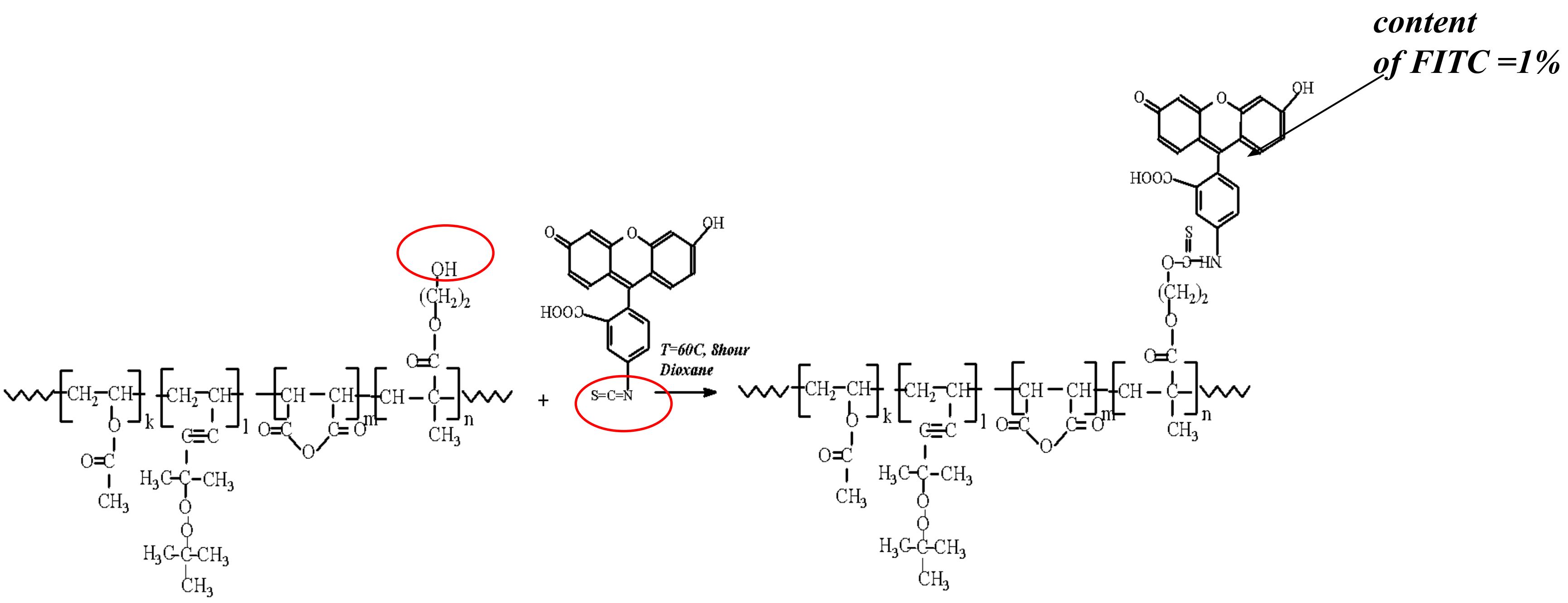

II.2. Synthesis of oligoperoxide and derived oligoelectrolyte surfactants containing luminescent organic fragments.

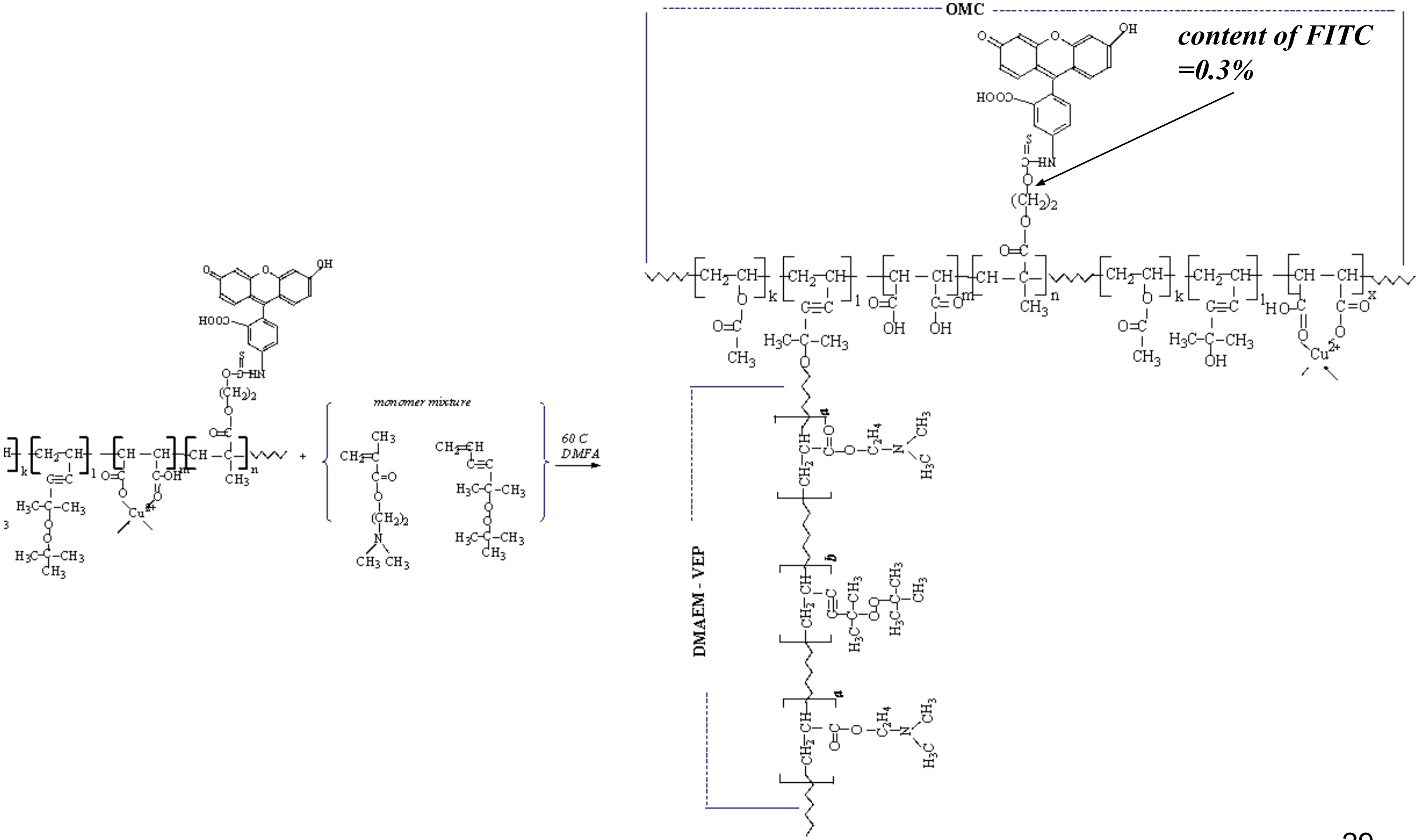

II.2. Synthesis of oligoperoxide and derived oligoelectrolyte surfactants containing luminescent fragments as a result of reactions with reactive phosphors.

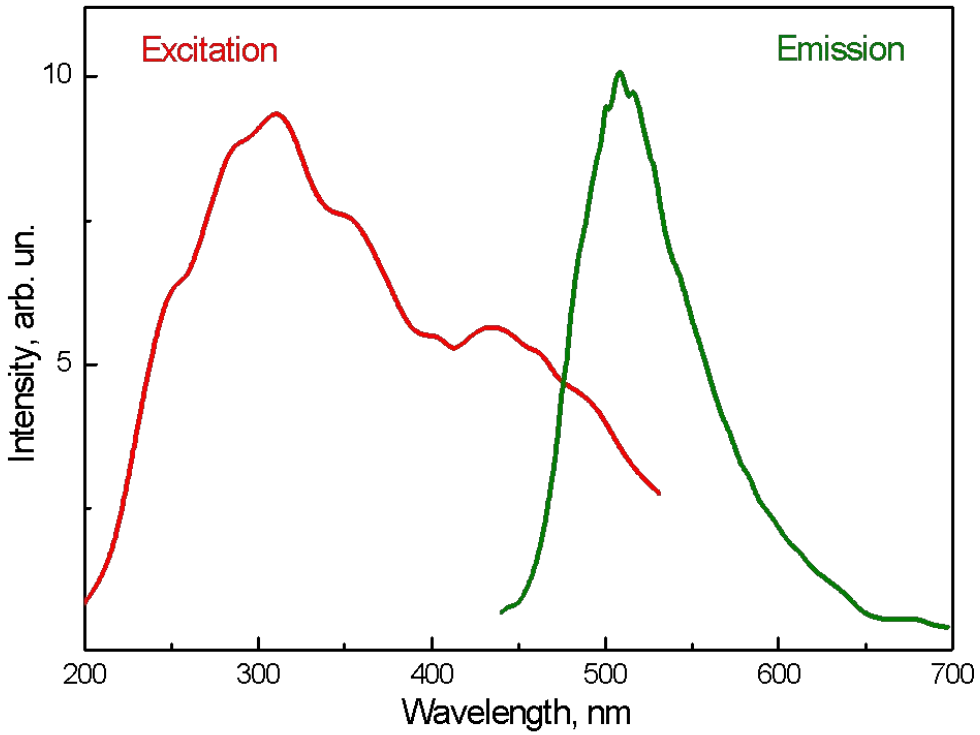

The excitation and emission spectra of VA-VEP-MA-HEMA+FITC-graft-VEP-DMAEM branched copolymer

II.2. Synthesis of oligoperoxide and oligoelectrolyte surfactants containing luminescent organic fragments.

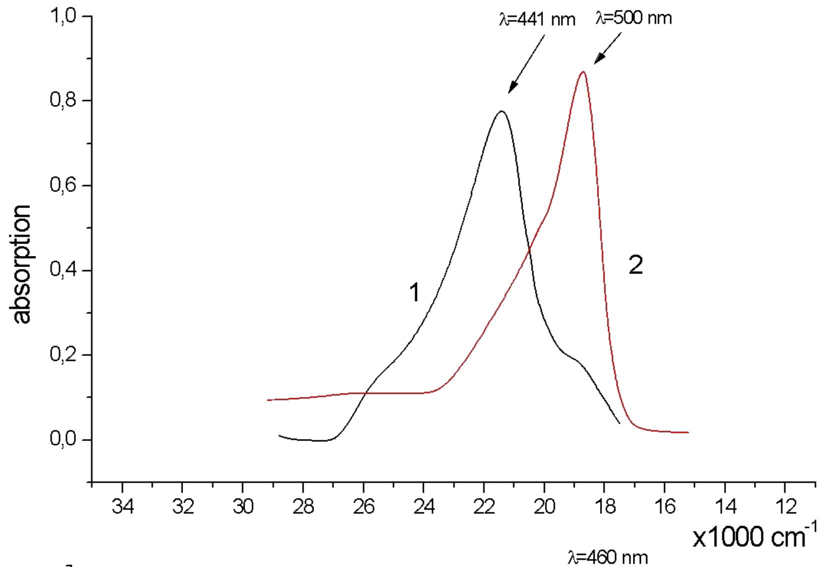

UV-spectra of FITC and copolymer with FITC fragments water solution (1) (2), pH=9

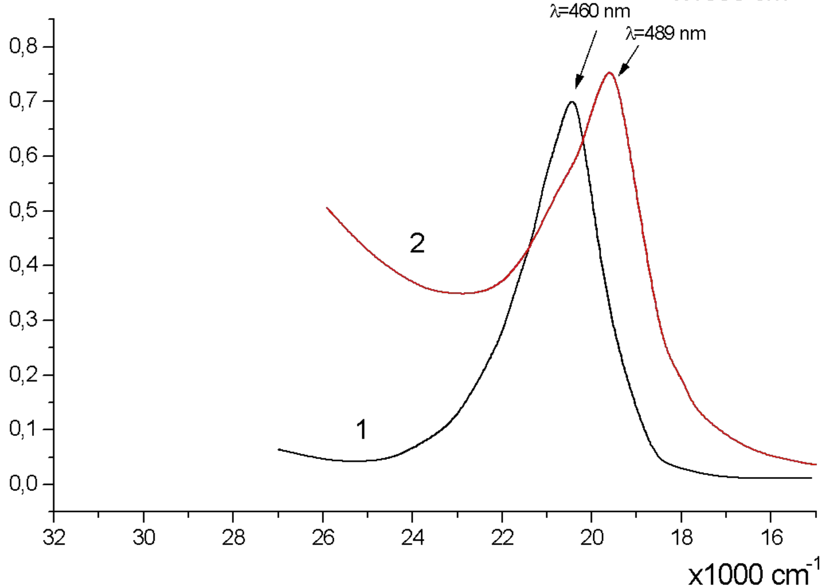

UV-spectra of FITC and comb- like copolymer with FITC fragments water solution (1) (2)

II.3. Micelle-like assemblies formed by oligoperoxide or oligoelectrolyte surfactants solubilizing organic phosphors in hydrophobic core.

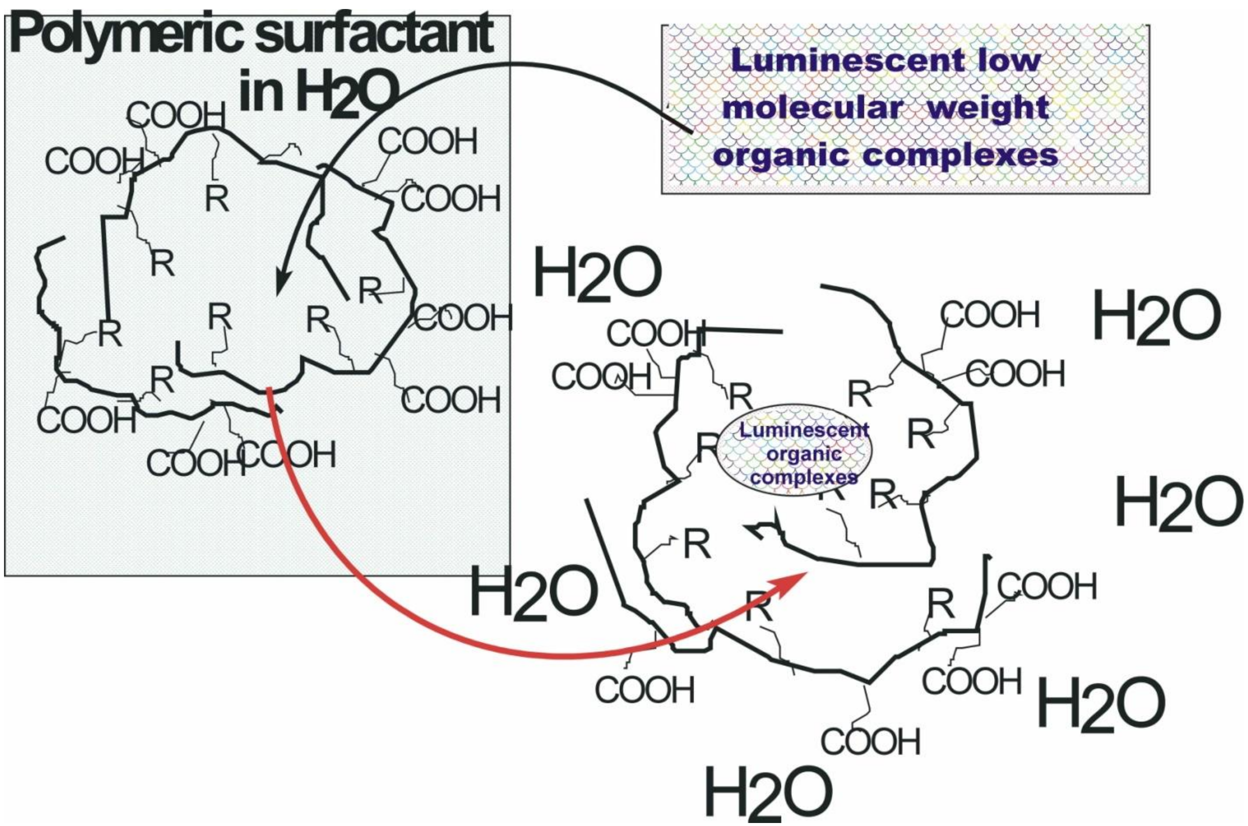

Scheme of solubilization of water-insoluble organic phosphors in the core of micelle forming oligoperoxide surfactants in water

II.3. Micelle-like assemblies formed by oligoperoxide or oligoelectrolyte surfactants solubilizing organic phosphors in hydrophobic core.

Coordinating metal complexes were synthesized by prof. S. Meshkova, Bogatskiy Physico-Chimical Institute of NASU

Eu $(TTA)_3$TFFO, where TTA - thenoyltrifluoroacetone, TFFO - tripheny iphosphineoxide

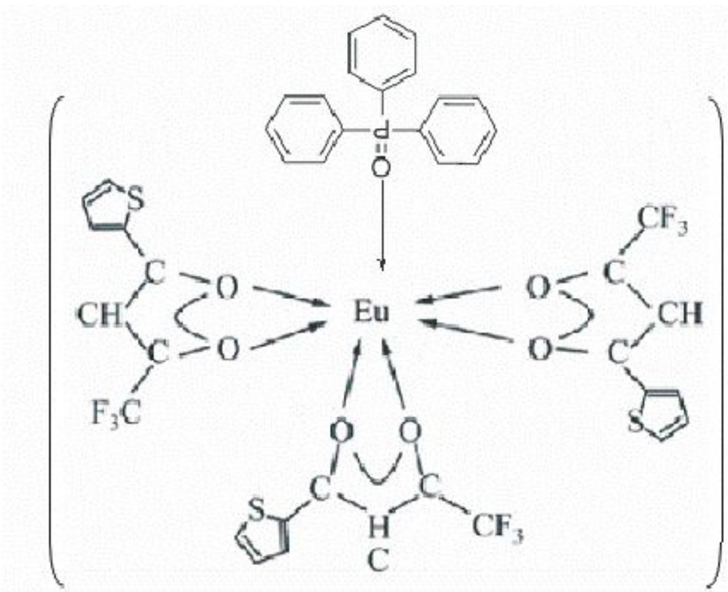

Tb$(AA)_3$TFFO, where AA - acetylacetonate, TFFO – triphenyl phosphineoxide,

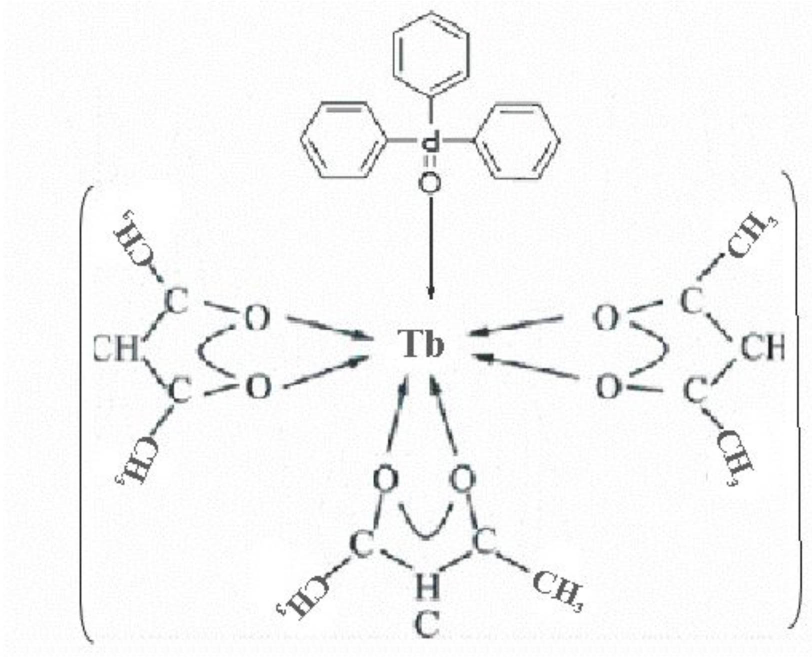

II.3. Micelle-like assemblies formed by oligoperoxide or oligoelectrolyte surfactants solubilizing organic phosphors in hydrophobic core.

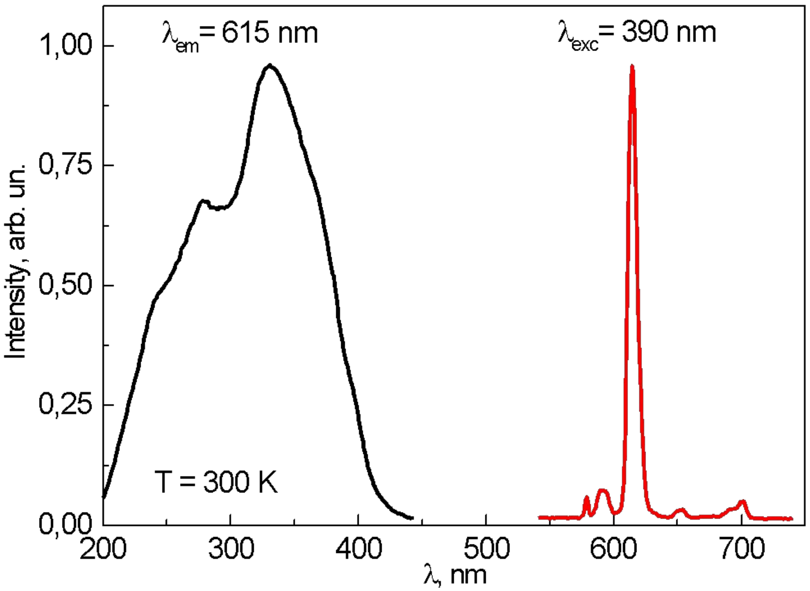

The excitation and emission spectra of Eu3+ for Eu (TTA) in the micelle hydrophobic zones of oliogoperoxide surfactants

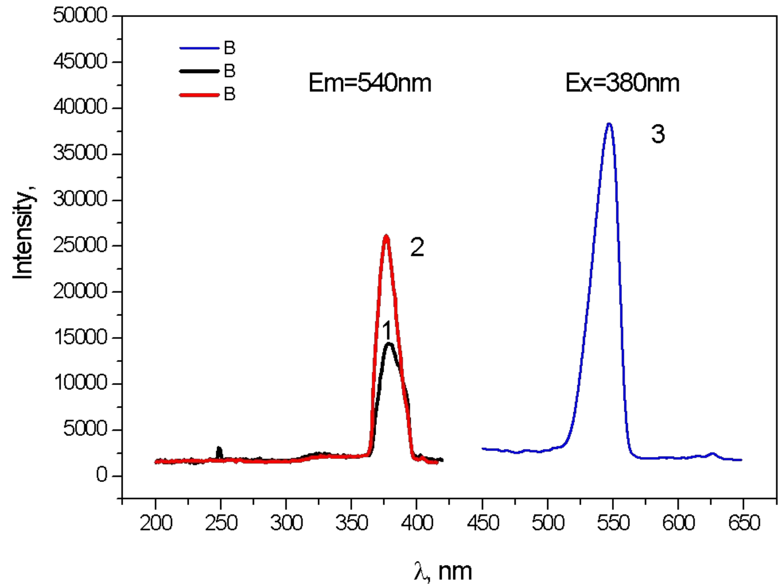

Spectra of excitation (1, 2) and luminescence (3) of the complex $Tb(AA)_3$ solubilized in micelles formed by oligo (VA-MAN-MP (T-3), concentration of the complex is 0.5% (1, 3) and 0.3% (2);

II.4. Oligoelectrolyte based nanogels containing coordinating rare earth cations or organic phosphors in the pores.

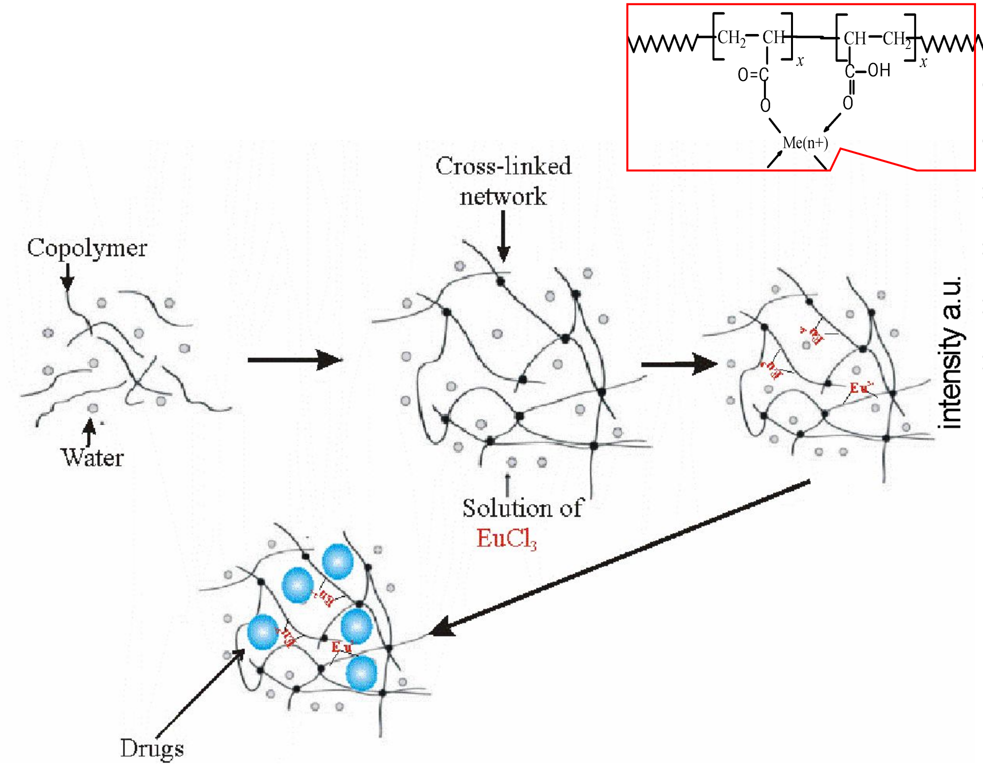

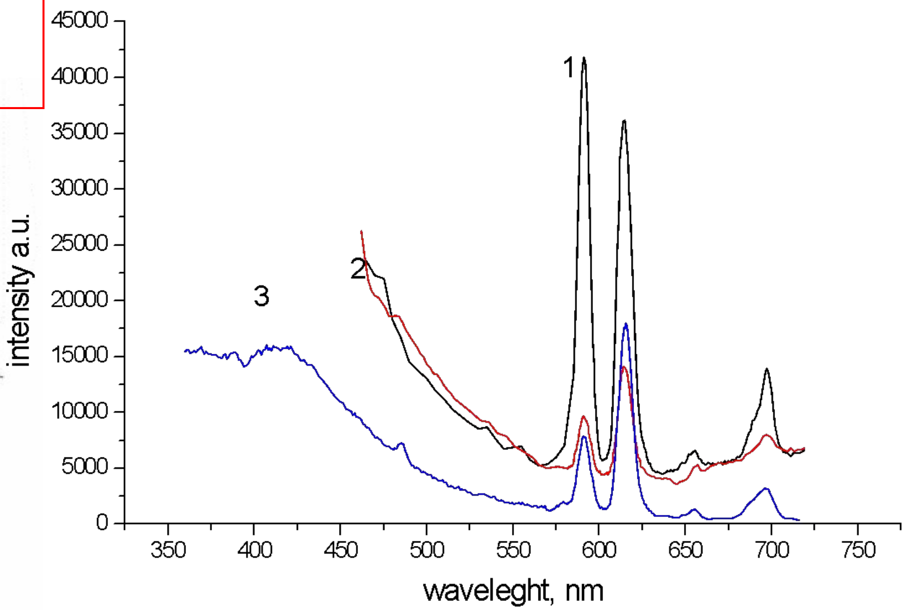

The scheme of the formation of luminescent carboxyl-containing gel carriers and loading poor water soluble drugs

Luminescent spectrum of coordinatung complex of Eu^{3+} with carboxyls of nanogel. Excitation at 397nm (1); 387nm - (2); 300nm – (3).

II.4. Oligoelectrolyte based nanogels containing coordinating rare earth cations or organic phosphors in the pores.

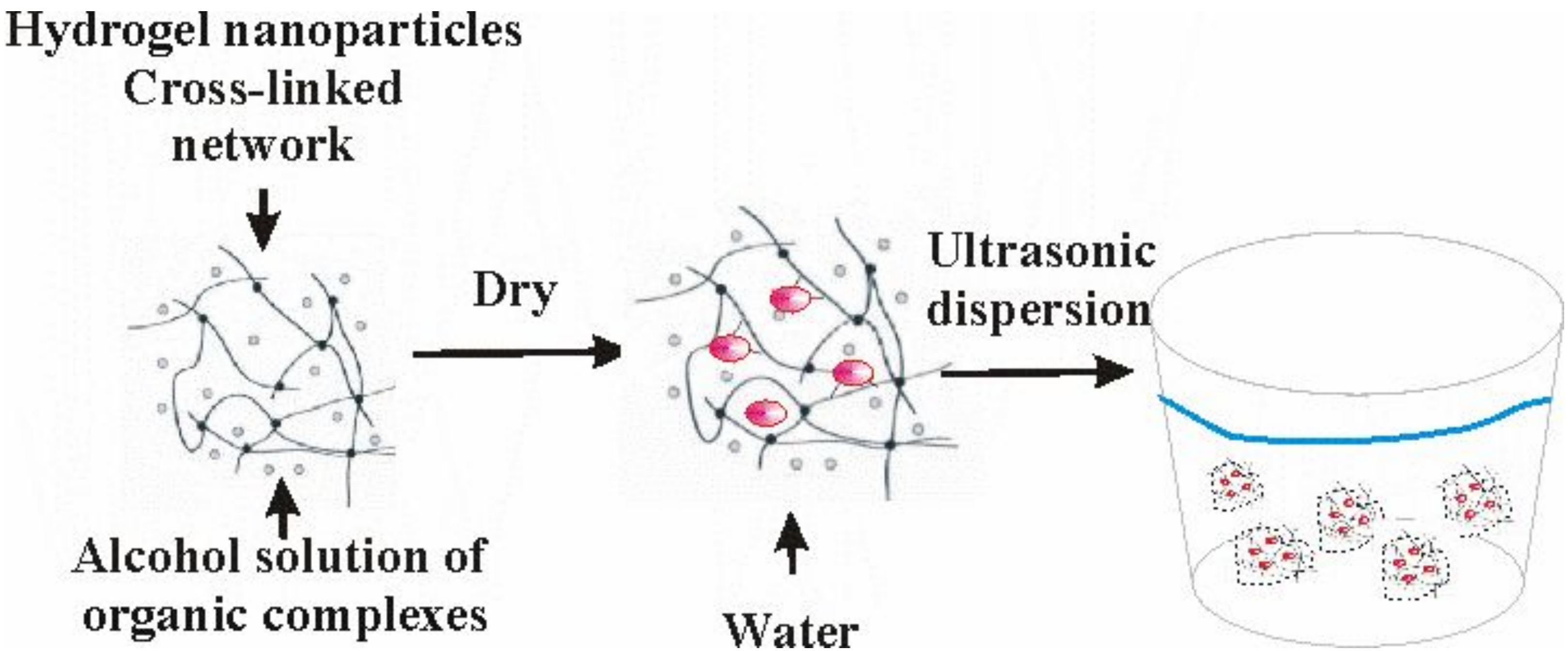

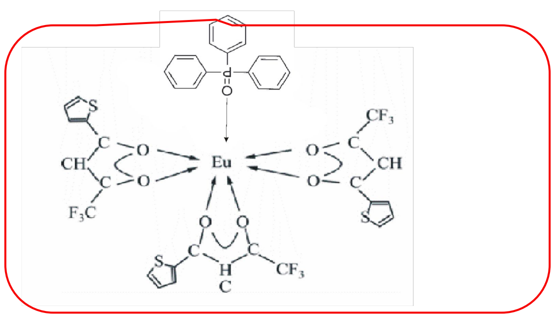

II.4. Oligoelectrolyte based nanogels containing coordinating rare earth cations or organic phosphors in the pores.

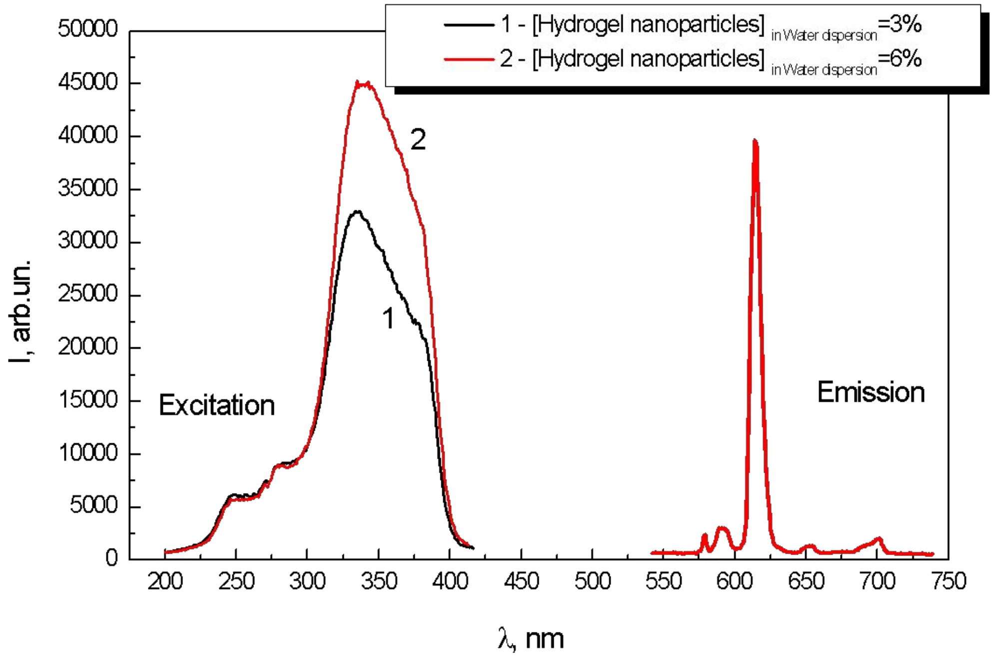

The excitation and emission spectra of nanogel water dispersions with the adsorbed complex Eu (TTA) 3TFFO, [nanogel]=3%(1) and 6% (2)([Eu (TTA)3·TFFO] =1% per nanogels)

Water dispersions of nanogels containing 3% (a), 1% (b), 0.5% (c) of complex $Eu(TTA)_3TFFO$

II.4. Oligoelectrolyte based nanogels containing coordinating rare earth cations or organic phosphors in the pores.

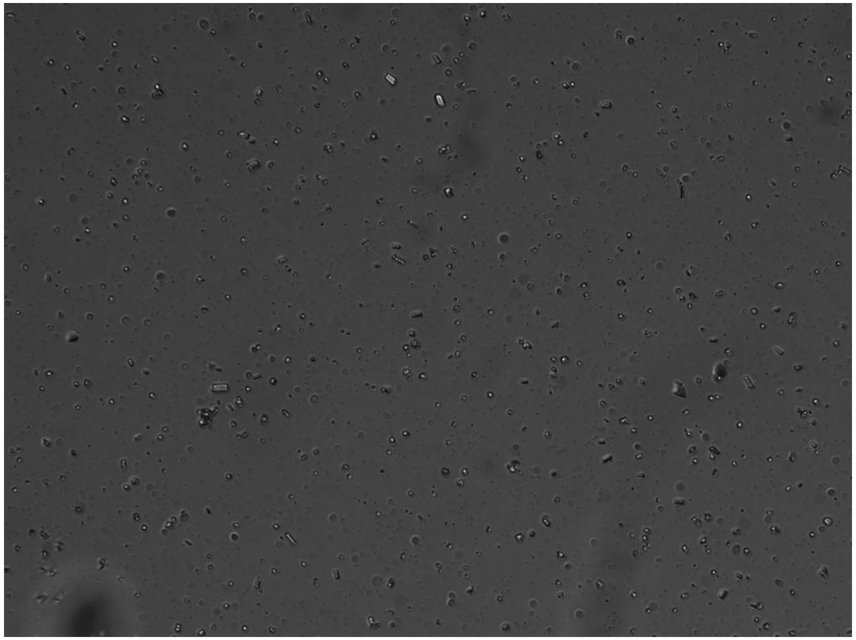

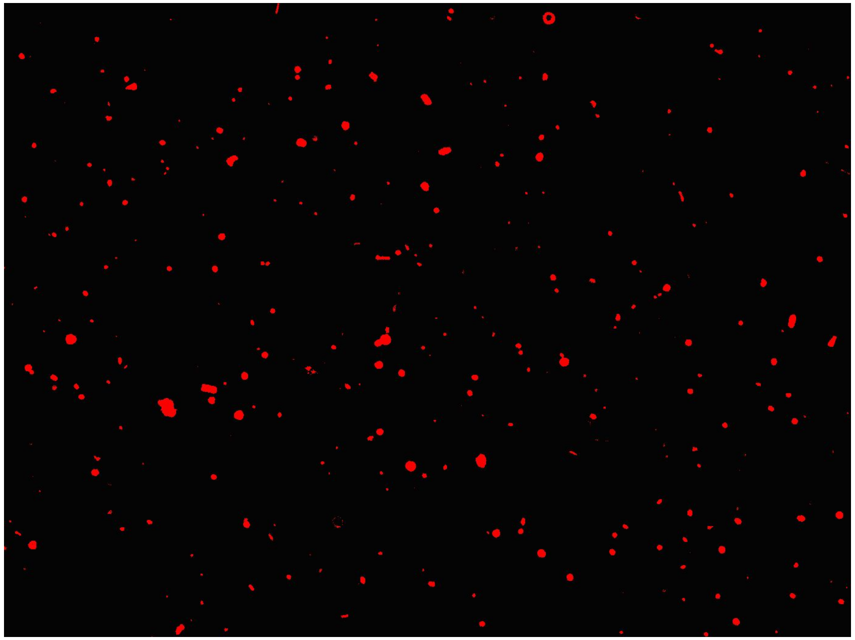

Optical microscope images of nanogels containing luminescent complex Eu (TTA)3·TFFO a) differential-interferential contrast, b) fluorescence

II.5. Encapsulation of phosphors in the core of functional polymeric nanoparticles via water dispersion polymerization.

Surface - active monomer (SAM)

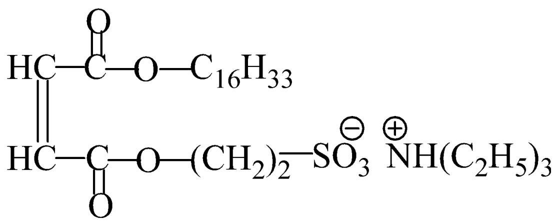

OMC

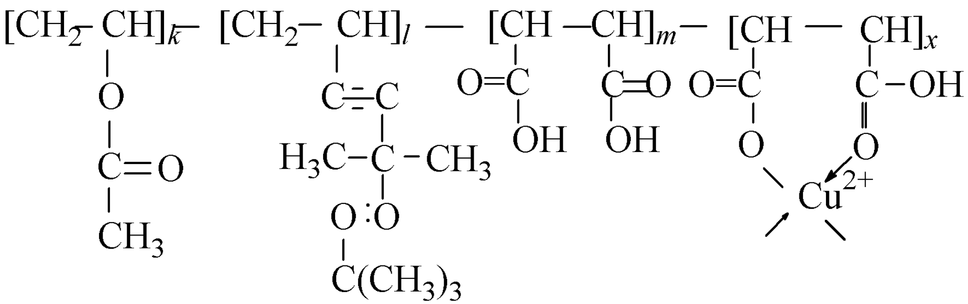

Fluorescent dyes

Water soluble

Fluorescein

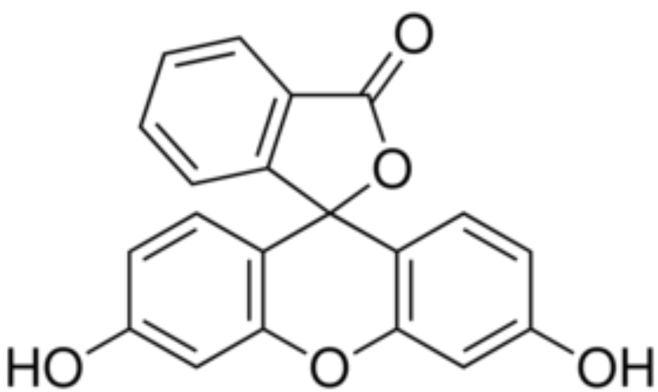

Water insoluble

2,6-Di-tert.-butyl-4-(2,5-diphenyl-3,4-dihydro-2H-pyrazol-3-yl)-phenol (pyrazolyne)

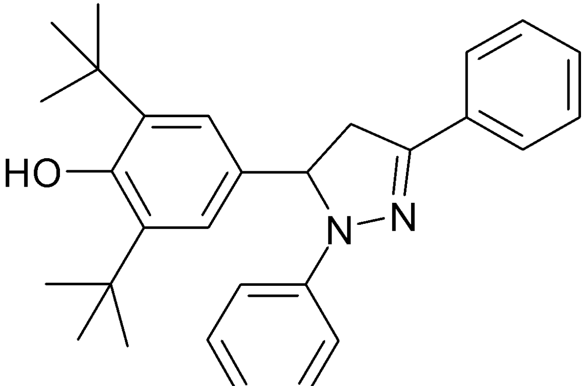

II.5. Encapsulation of phosphors in the core of functional polymeric nanoparticles via water dispersion polymerization.

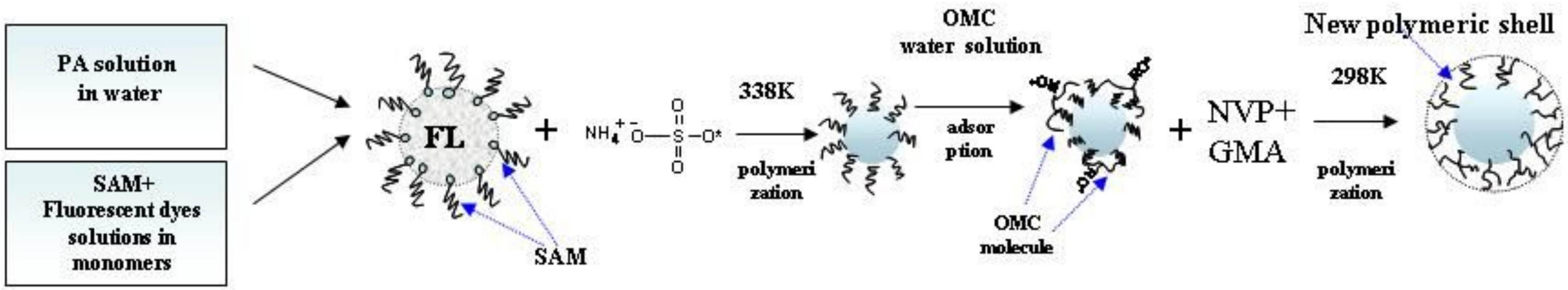

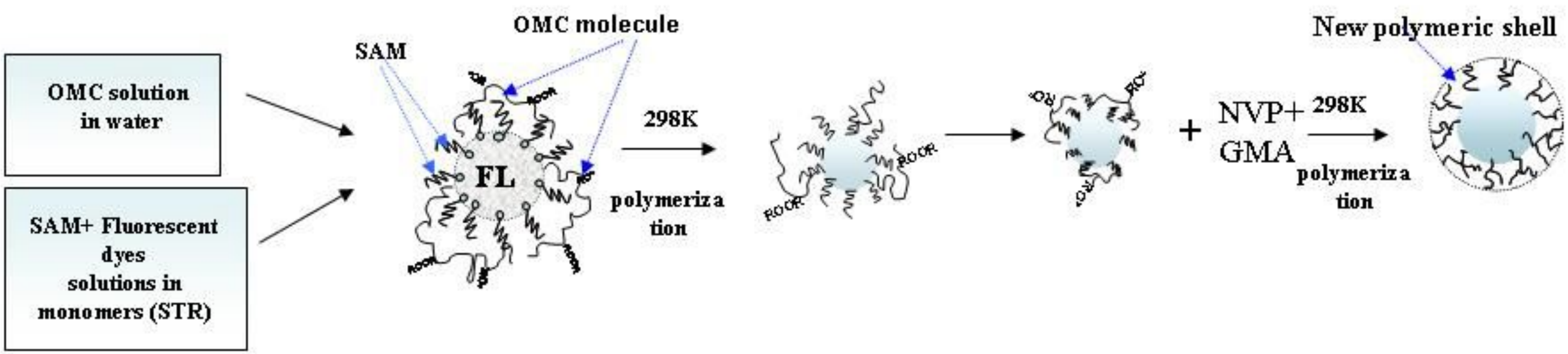

II.5. Encapsulation of phosphors in the core of functional polymeric nanoparticles via water dispersion polymerization.

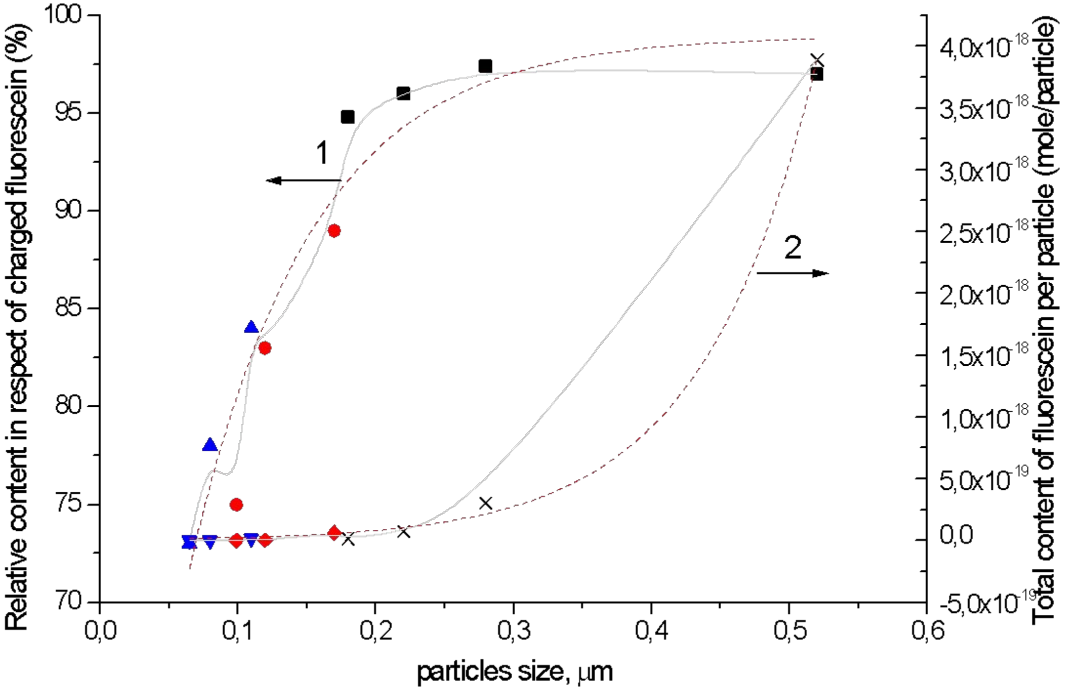

The dependences of relative in respect of charged amount (1) and total (2) contents of fluorescein encapsulated per one functional nanoparticle on nanoparticle size. (■,×– monomer mixture: STR:SAM, initiator – PA, ●,♦– monomer mixture: STR:SAM, initiator – OMC, ▲,▼– monomer mixture: MMA-BA-GMA:SAM, initiator – OMC)

II.5. Encapsulation of phosphors in the core of functional polymeric nanoparticles via water dispersion polymerization.

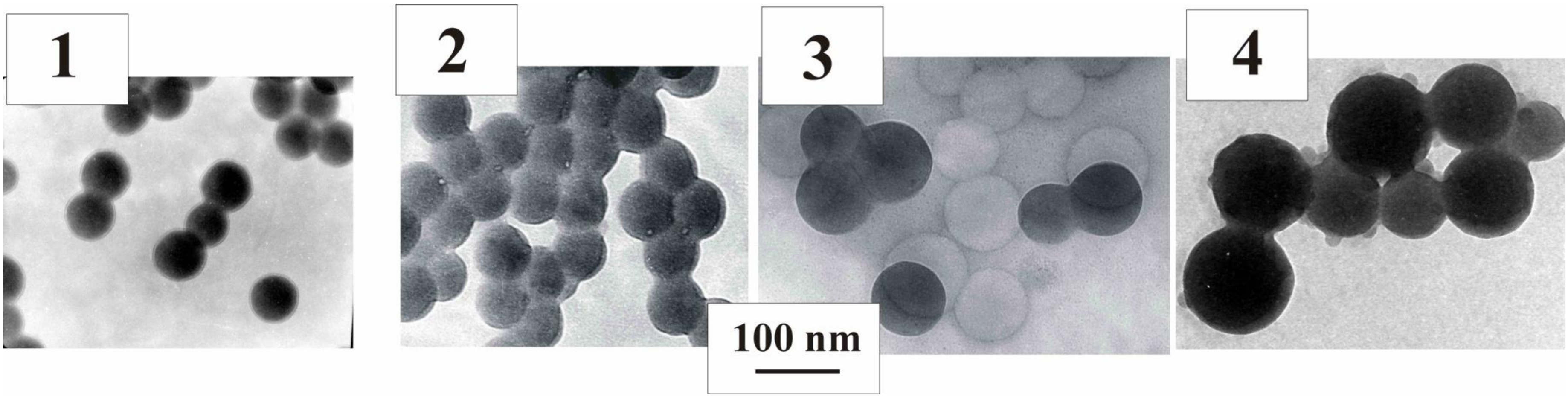

TEM images of functional polymeric NPs synthesized via water dispersion polymerization of styrene with SAM at St: SAM ratio 90:10 initiated by OMC: 1 – without fluorescein (FL), 2 – [FL] =0.1% per St, 3 – [FL] =0.5% per St, and initiated by PA, [FL] =0.1% per St (3)

II.5. Encapsulation of phosphors in the core of functional polymeric nanoparticles via water dispersion polymerization.

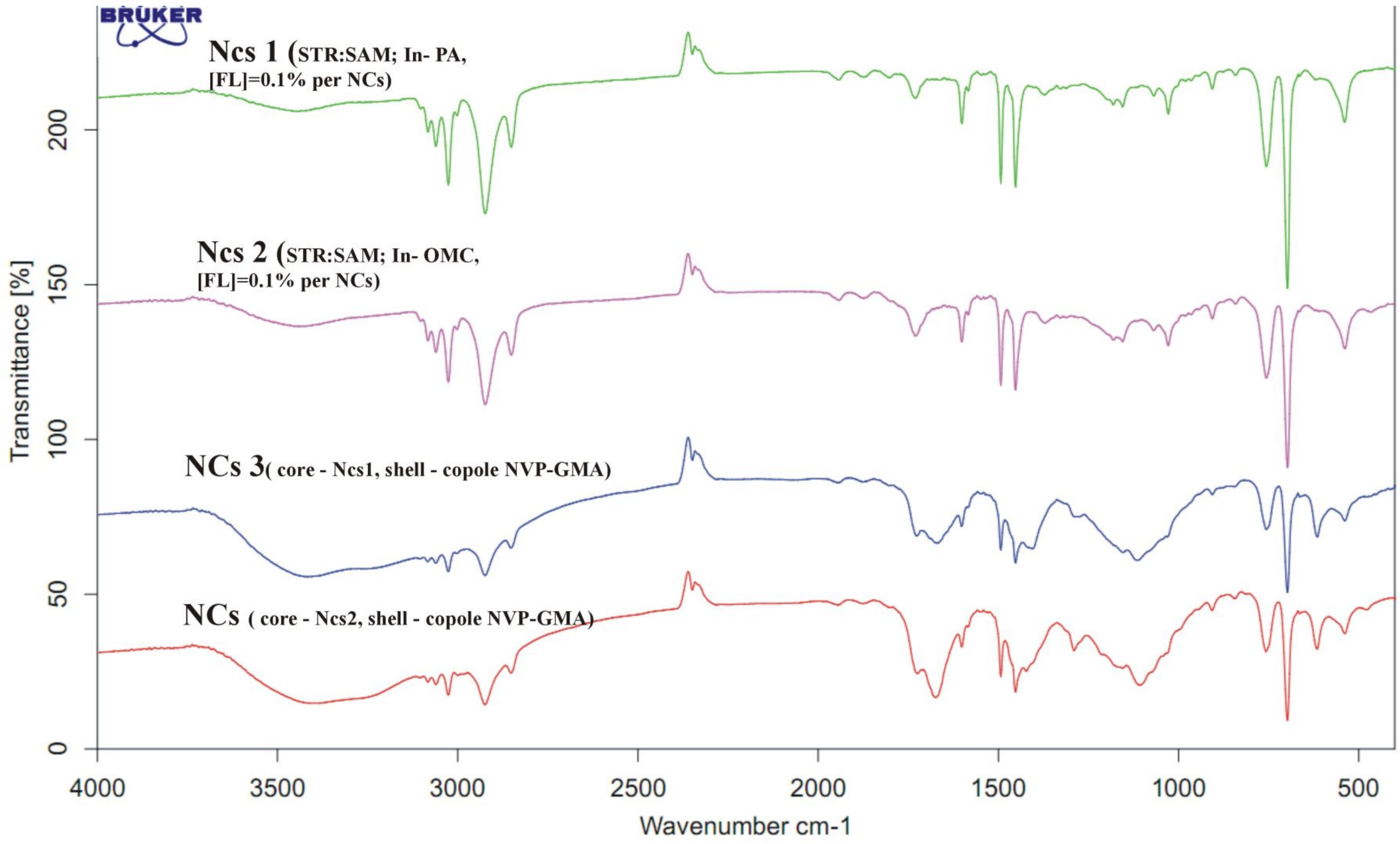

FT-IR spectrum of polymeric NPs containing encapsulated fluorescein, copolymer of St and SAM (1, 2) and core-shell type NPs (3,4)

II.5. Encapsulation of phosphors in the core of functional polymeric nanoparticles via water dispersion polymerization.

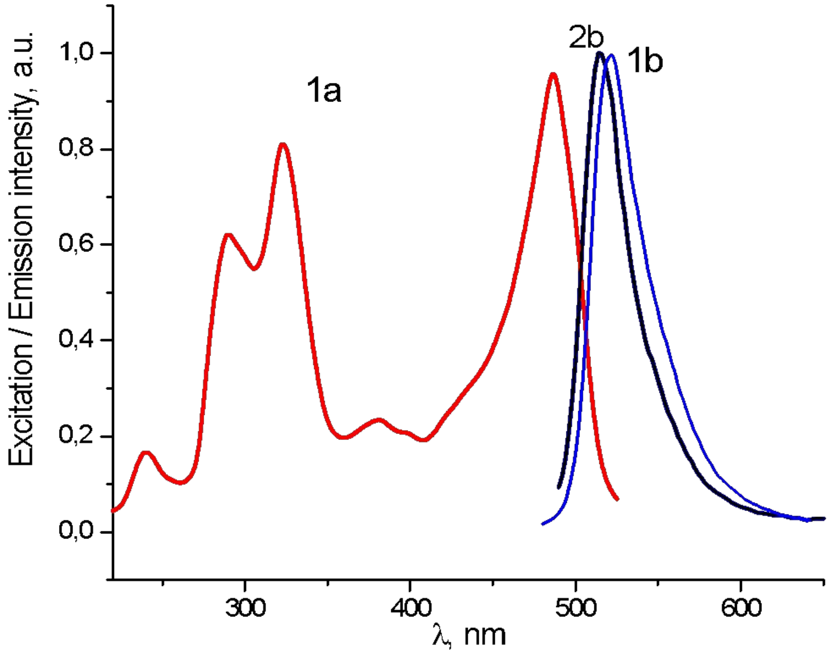

Fluorescence (1) and fluorescence excitation (2) spectra of polymeric fluorescein-encapsulated NPs. b – Emission spectra of fluorescein (1) and of fluorescein-encapsulated NPs (2); excitation at 425 nm.

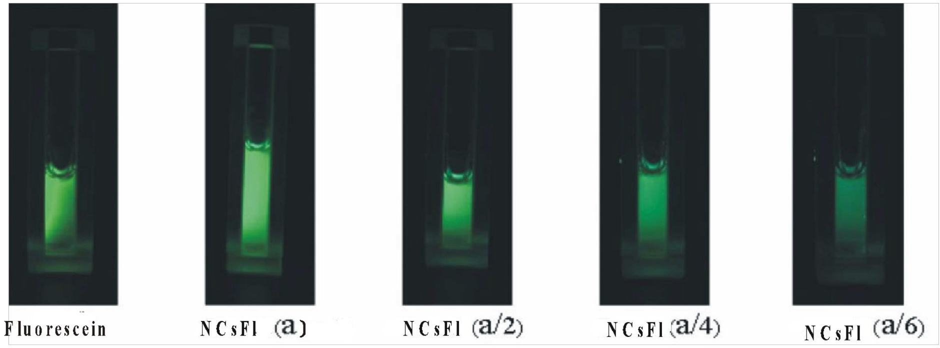

Green fluorescence of FITS and FITC-encapsulated polystyrene nanoparticles (PSFITS a) in water based systems at distinct dilution (PSFITS a/2, a/4, a/6)

II.5. Encapsulation of phosphors in the core of functional polymeric nanoparticles via water dispersion polymerization.

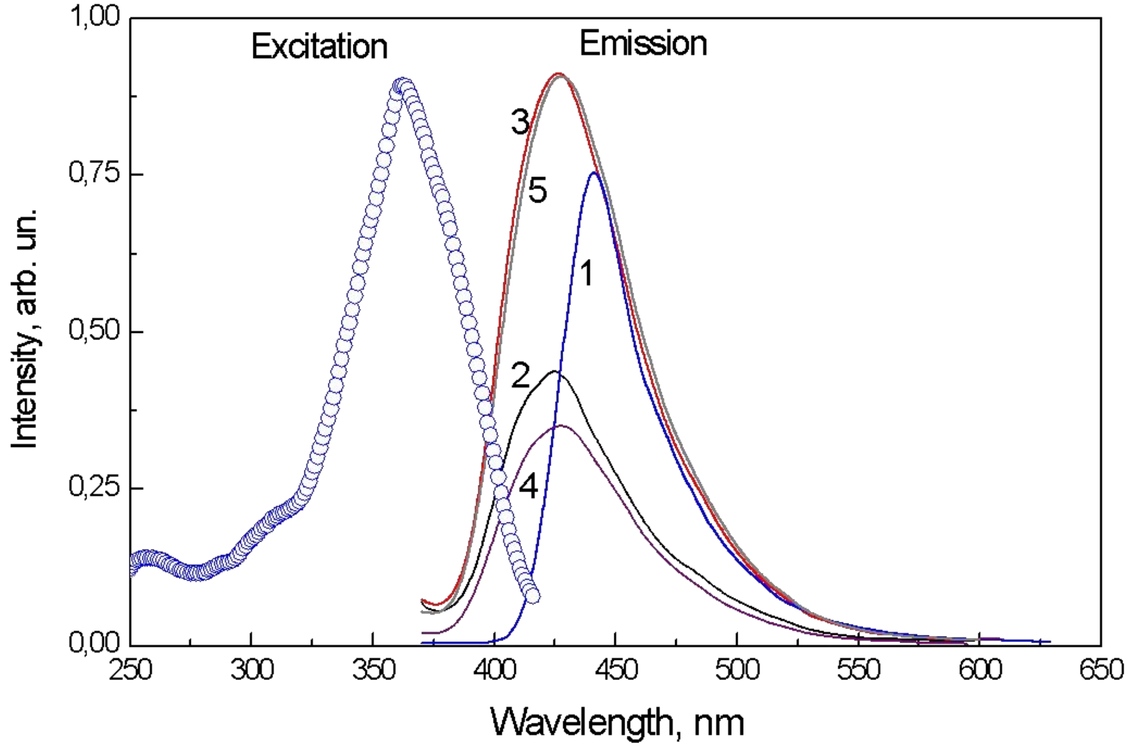

Spectrum of excitation and emission of pyrazolyne in toluene (1) and water dispersions of pyrazolyne-encapsulated polymeric nanoparticles : 2, 3 – polystyrene: SAM; 4, 5 – the same nanoparticles after grafting polymeric chain of MMA-BA-GMA; [dye] =0.1% per polymer (2, 4) and 0.05% per polymer (3, 5).

II.5. Encapsulation of phosphors in the core of functional polymeric nanoparticles via water dispersion polymerization.

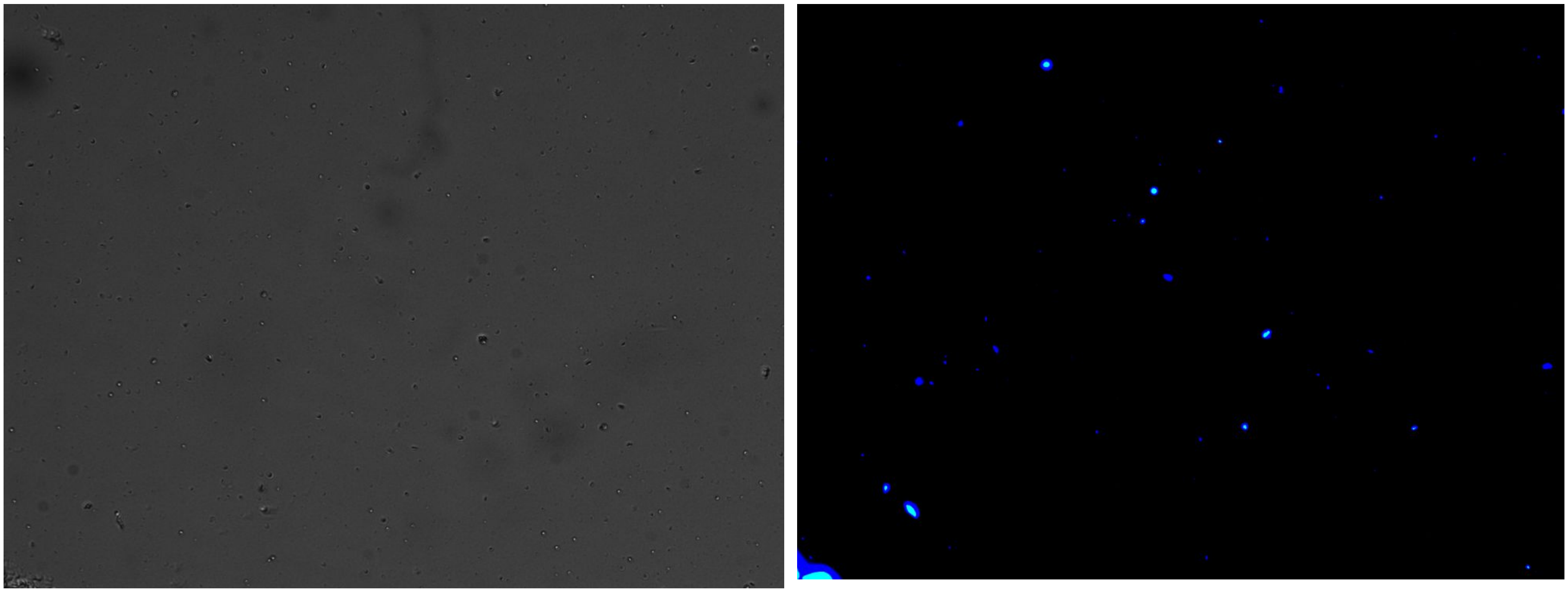

Optical microscope images of pyrazolyne-encapsulated polystyrene NPs. a) differential-interferential contrast, b) fluorescence

II.6. Functional mineral nanoparticles of $LaPO_4$, $LuPO_4$, $LuBO_3$, GdF_3, CaF_2, BaF_2 core doped with cations of Pr^{+3}, Ce^{+3}, Eu^{+2}, Eu^{+3}.

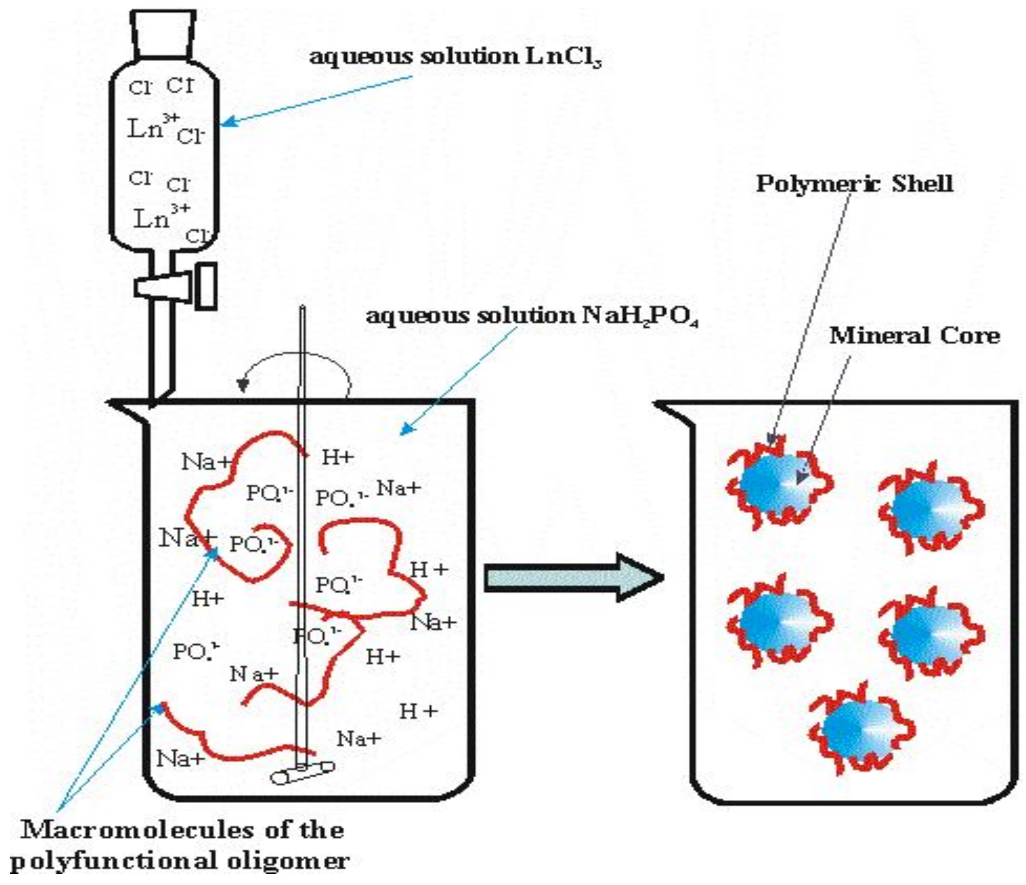

The scheme of the lantanide nanoparticle template synthesis

II.6. Functional mineral nanoparticles of $LaPO_4$, $LuPO_4$, $LuBO_3$, GdF_3, CaF_2, BaF_2 core doped with cations of Pr^{+3}, Ce^{+3}, Eu^{+2}, Eu^{+3}.

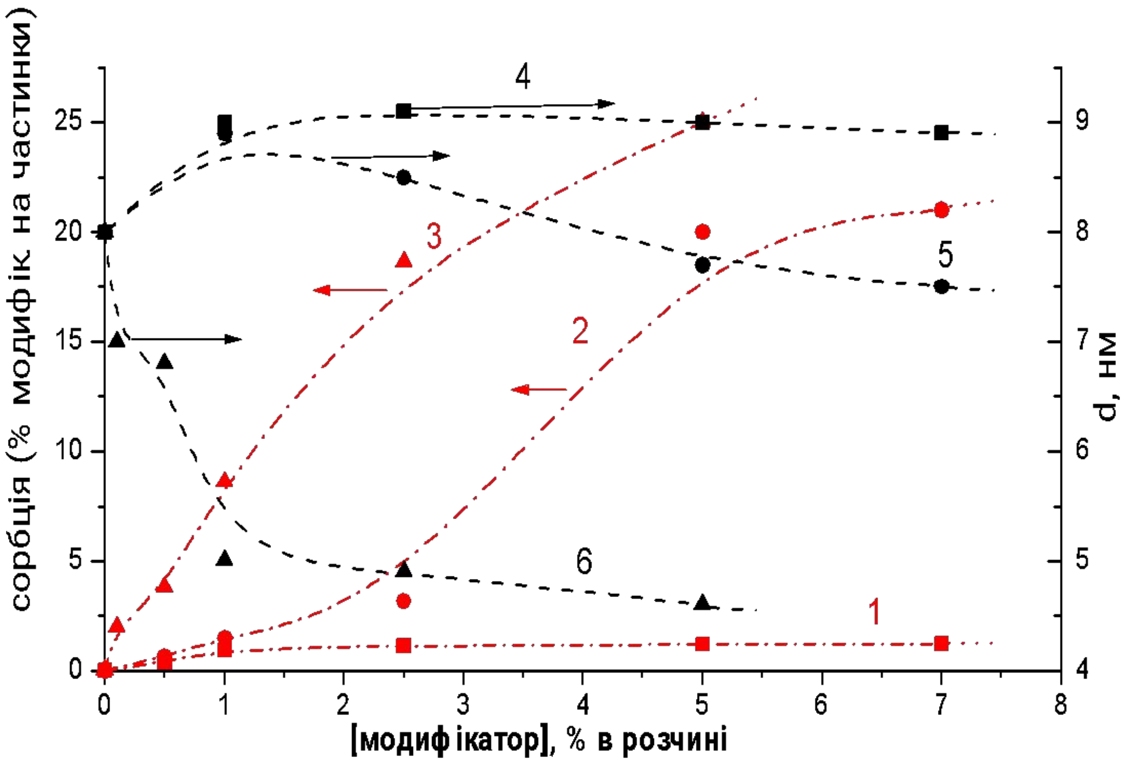

The dependence of oligoperoxide adsorption value (1, 2, 3) and $LaPO_4$…Eu^{3+} nanocrystal size (4, 5, 6) formed as a result of nucleation in the presence of oligoperoxide surfactant: 1 – rycinox, 2- oligo(NVP-co-VEP-co-GMA); 3 –oligo(VA-co-VEP-co-MAN)

II.6. Functional mineral nanoparticles of $LaPO_4$, $LuPO_4$, $LuBO_3$, GdF_3, CaF_2, BaF_2 core doped with cations of Pr^{+3}, Ce^{+3}, Eu^{+2}, Eu^{+3} and oligoperoxide shell.

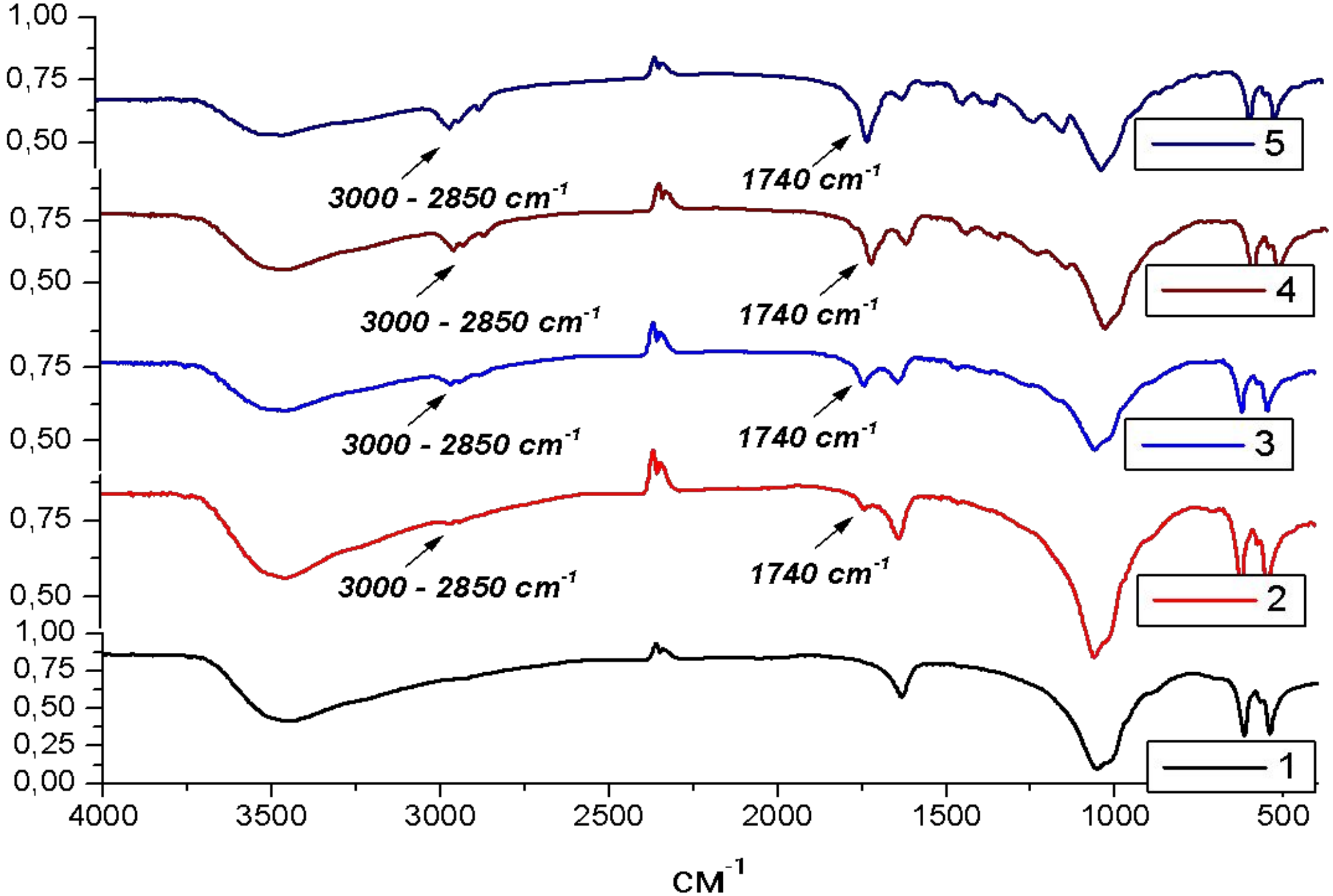

FT-IR spectrum of $LaPO_4$…Eu^{3+} nanoparticles obtained without oligoperoxide surfactant (1) and obtained in the presence of oligo(VA-co-VEP-co-MA): 0.1% (2), 0.5% (3), 1% (4) and 5% (5)

II.6. Functional mineral nanoparticles of $LaPO_4$, $LuPO_4$, $LuBO_3$, GdF_3, CaF_2, BaF_2 core doped with cations of Pr^{+3}, Ce^{+3}, Eu^{+2}, Eu^{+3}.

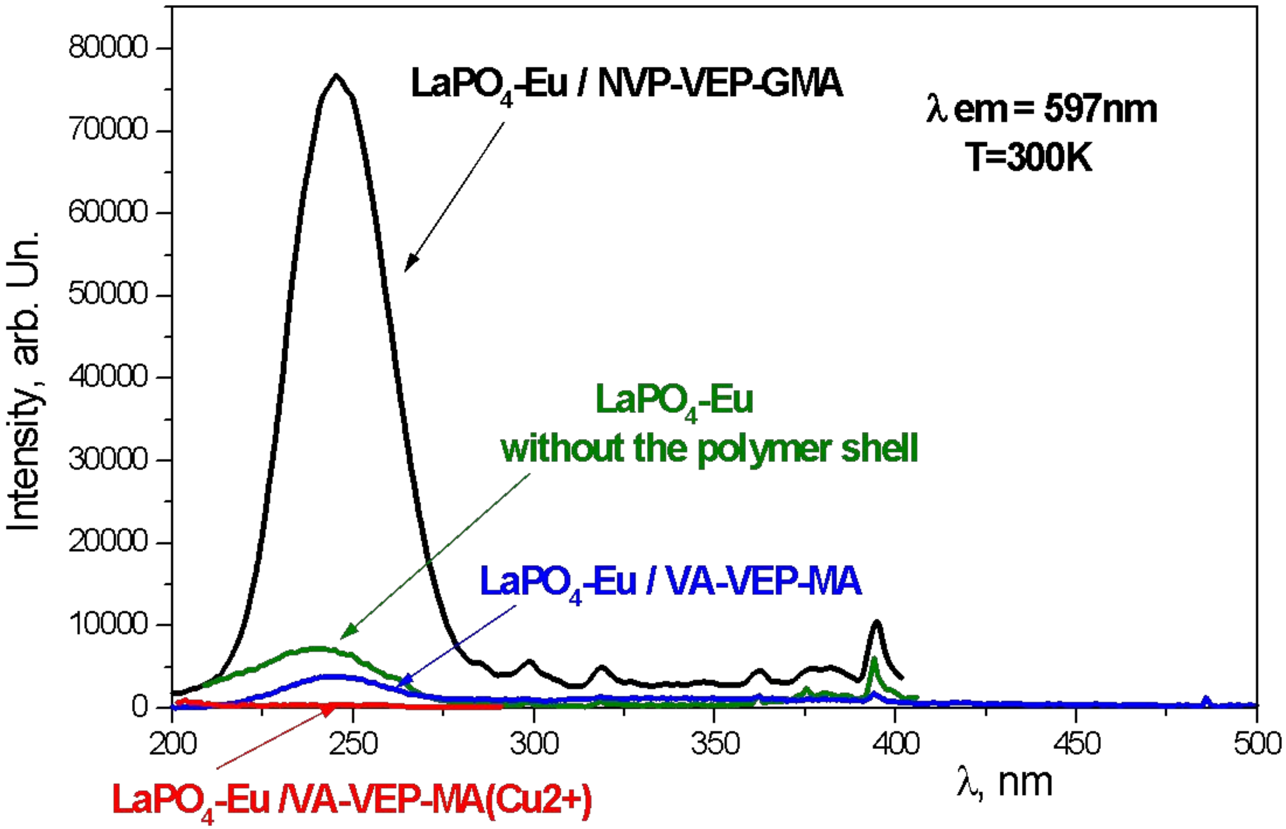

Influence of the nature of oligoperoxide shell on the surface of nanoparticles on intensity of their luminescence

II.6. Functional mineral nanoparticles of $LaPO_4$, $LuPO_4$, $LuBO_3$, GdF_3, CaF_2, BaF_2 core doped with cations of Pr^{+3}, Ce^{+3}, Eu^{+2}, Eu^{+3}

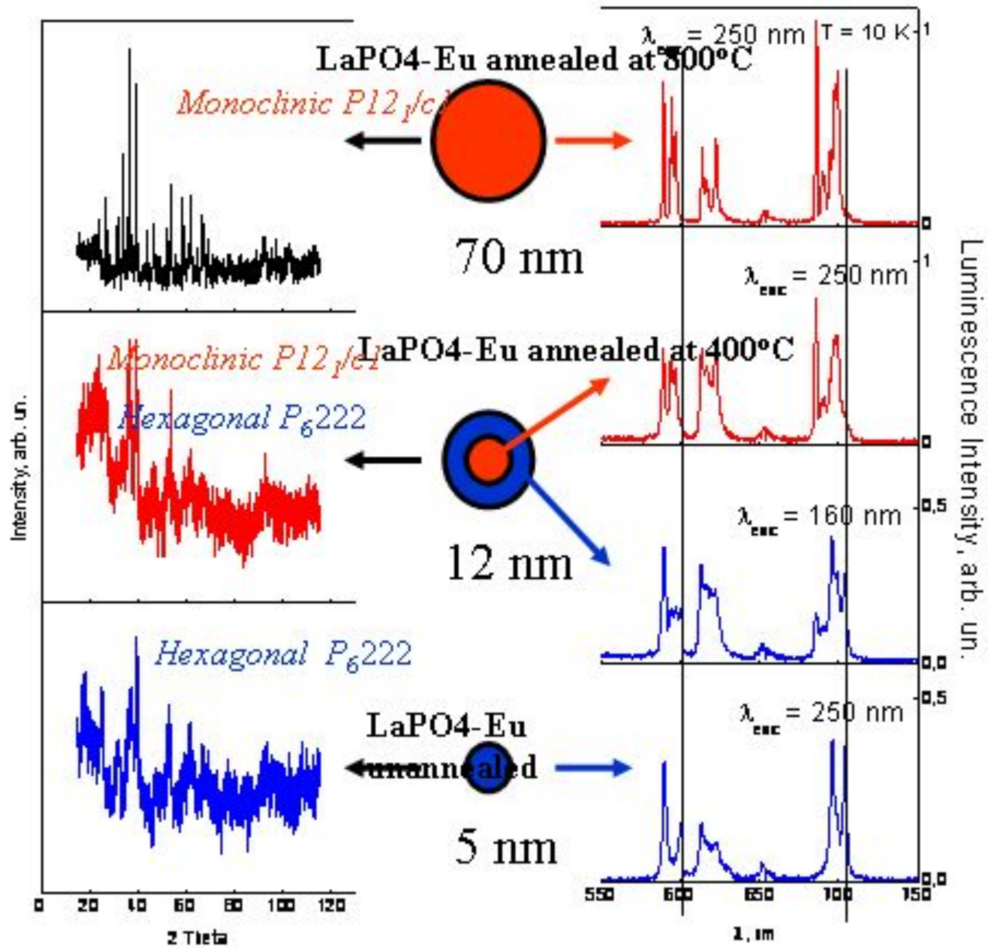

X-Ray patterns of nanoparticles $LaPO_4$-Eu

The luminescence spectra of nanoparticles $LaPO_4$-Eu; T=10 K.

X-ray patterns of $LaPO_4$…Eu^{3+} nanoparticles annealed at different temperature (a) and spectrum of their luminescence (b): hexagonal lattice (blue) and monoclinic lattice (red)

II.6. Functional mineral nanoparticles of $LaPO_4$, $LuPO_4$, $LuBO_3$, GdF_3, CaF_2, BaF_2 core doped with cations of Pr^{+3}, Ce^{+3}, Eu^{+2}, Eu^{+3}

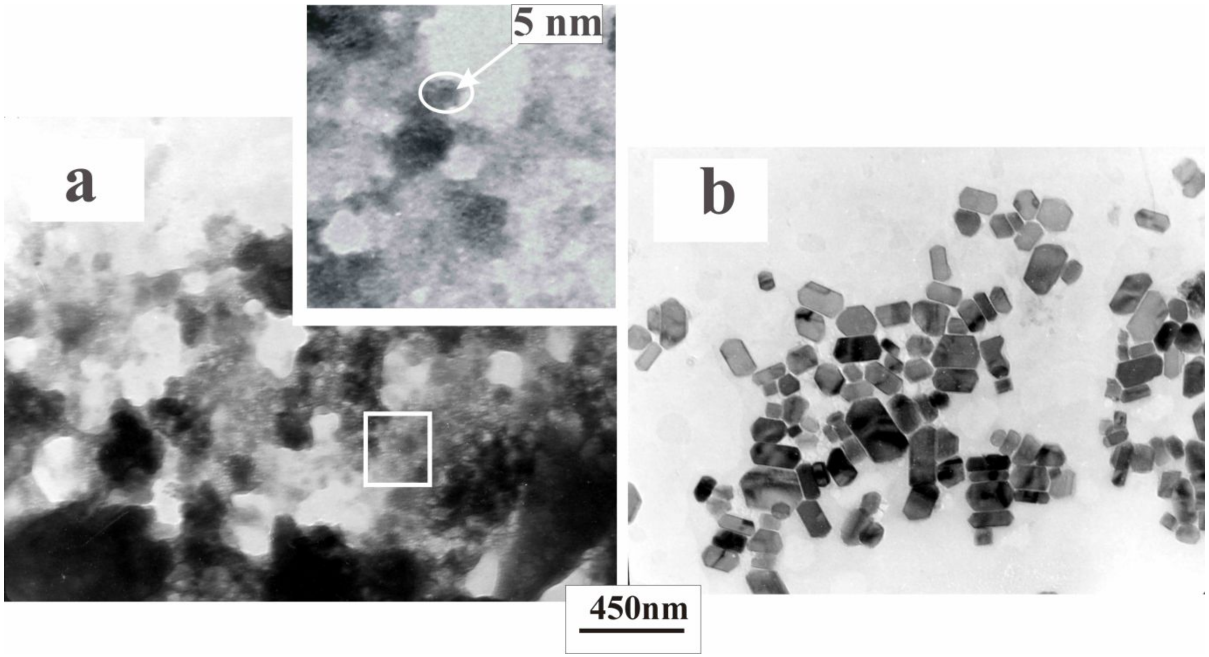

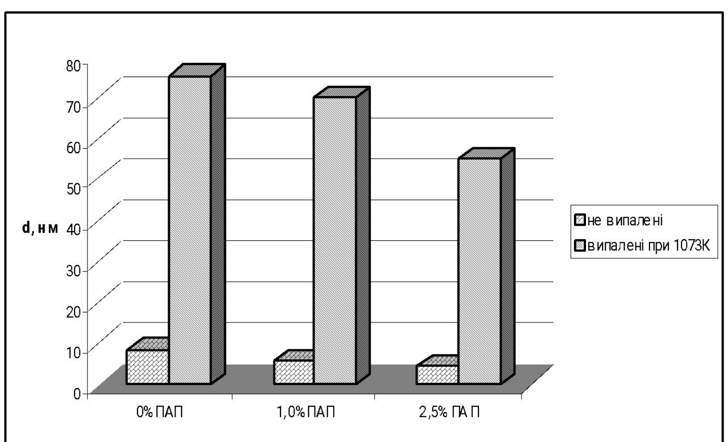

The dependence of the size of $LaPO_4$…Eu^{3+} nanoparticles non annealed and annealed at 1073K on oligoperoxide surfactant concentration in the solution during their nucleation

II.6. Functional mineral nanoparticles of $LaPO_4$, $LuPO_4$, $LuBO_3$, GdF_3, CaF_2, BaF_2 core doped with cations of Pr^{+3}, Ce^{+3}, Eu^{+2}, Eu^{+3}

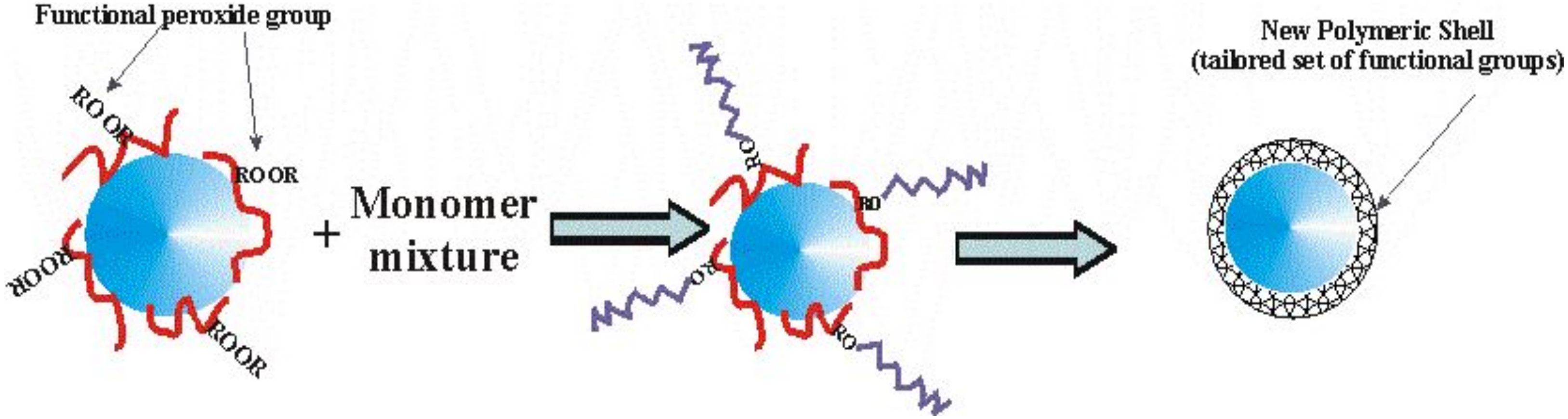

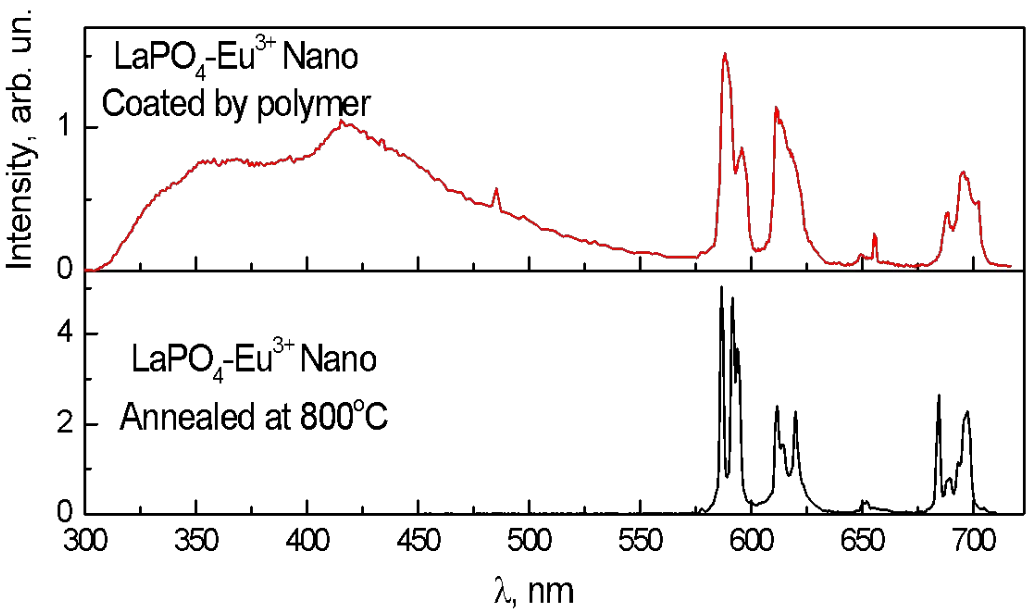

Lumenation Spectrum of $LnPO_4$ uncoated nanoparticles and coated nanoparticles

II.6. Functional mineral nanoparticles of $LaPO_4$, $LuPO_4$, $LuBO_3$, GdF_3, CaF_2, BaF_2 core doped with cations of Pr^{+3}, Ce^{+3}, Eu^{+2}, Eu^{+3}

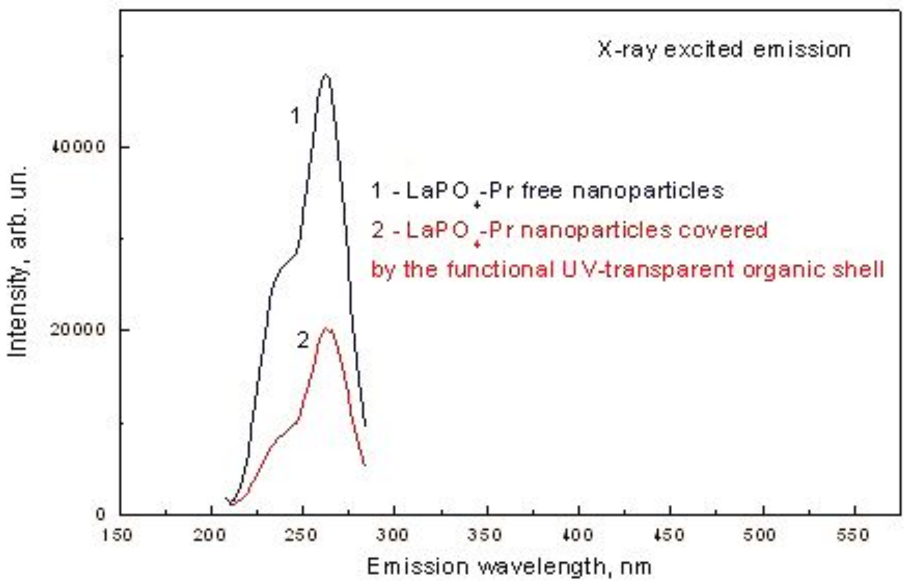

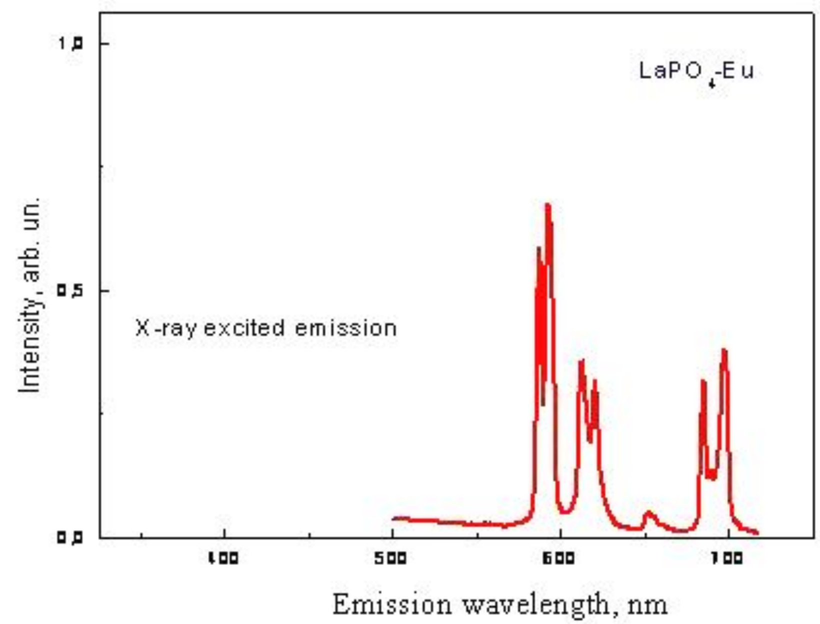

Spectrum of X-ray excited nanoparticles $LaPO_4$…Pr and LaPO4…Eu annealed at 800C (1) and the same nanoparticles after adsorption activation with oligoperoxide surfactant and subsequent radical grafting polystyrene shell (2)

II.7. Luminescent nanolayers on flat plate surfaces deposited from solutions and dispersions of functional polymeric and polymer-mineral nanocomposites.

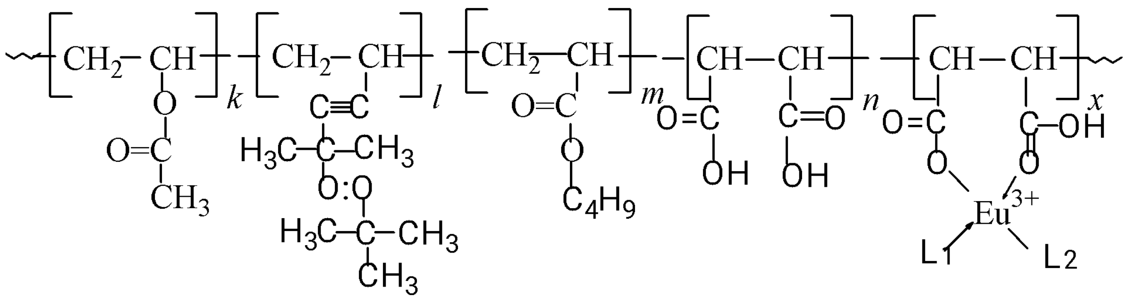

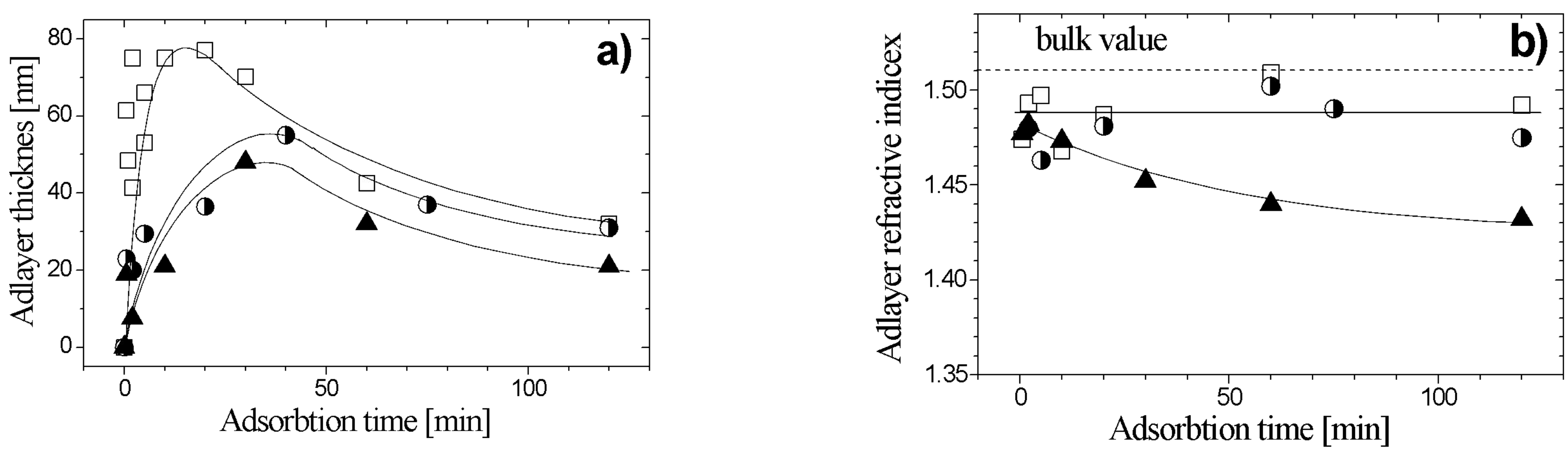

An average thickness (a) and refractive index (b) determined with ellipsometry for PO-Eu adlayers as a function of adsorption time for OP-Eu solutions with concentration: 0.6 % (triangles), 1.0 % (circles) and 2.5 % (squares). Solid lines are a guide to eye. Dashed line in (b) denotes bulk value extrapolated from solution refractometry

II.7. Luminescent nanolayers on flat plate surfaces deposited from solutions and dispersions of functional polymeric and polymer-mineral nanocomposites.

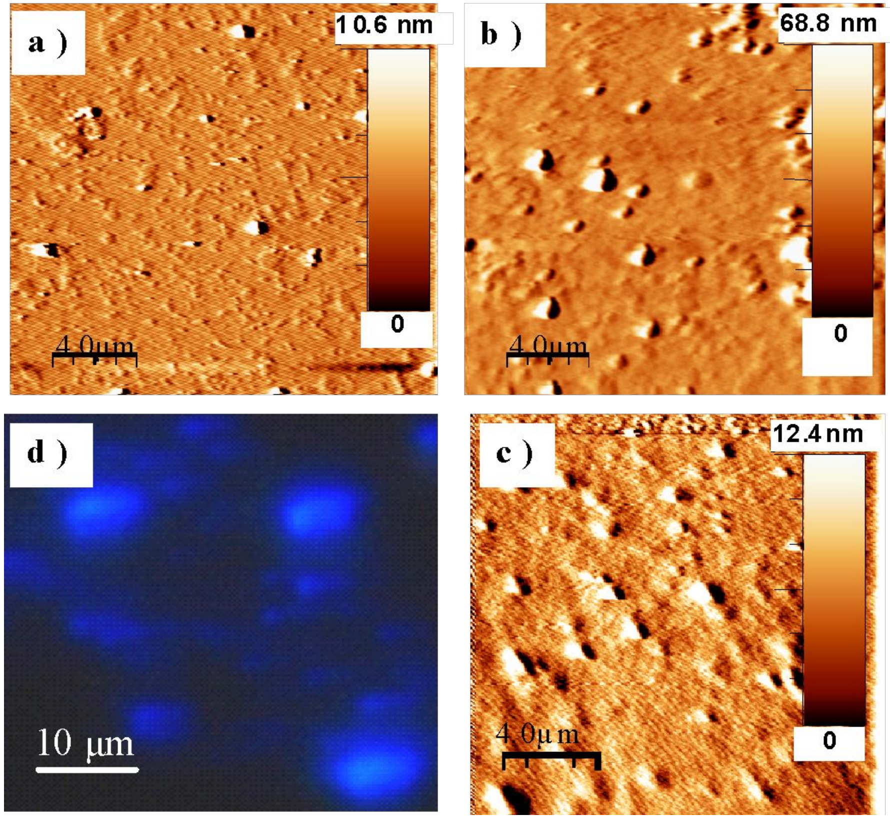

AFM (a-c) and fluorescence (d) micrographs of glass surfaces without (a) and with OP-Eu complexes (b-d) adsorbed from 0.6 % (b) and 2.5 % (c, d) water-ammonia solutions for 5 min (b-c). Surfaces are characterized by adlayer thickness 0 (a), ~20 nm (b) and 60 nm (c); rms roughness of 1.2 nm (a), 11 nm (b) and 2.1 nm (c); and effective fraction of area modified by OP-Eu complexes x equal to 0 (a), ~31 % (b) and ~90 % (c).

Why such oligoperoxide based luminescent nanocomposites and nanolayers?

- Controlled particle size and size distribution
- Controlled functionality and reactivity
- Controlled physically detectable characteristics of nanocomposites and nanoshells
- Presence of peroxide links on particle surface provides tailored particle functionalization (epoxide, aldehyde, maleimide etc.) via graft copolymerization.
- Availability of controlled reactive functionality on nanoparticle surface provides attachment of cell recognizing biological vectors (saccharides, lectins, antibodies).

III. Cellular studies and potential biomedical application for pathological cell detection, tagging and treatment.

*** Cellular study was fulfilled in Lviv Institute of Cell Biology under the guidance of Professor R. Stoika**

The ideal structure of multifunctional nanosized carriers for diagnostics, drug delivery and targeted treatment

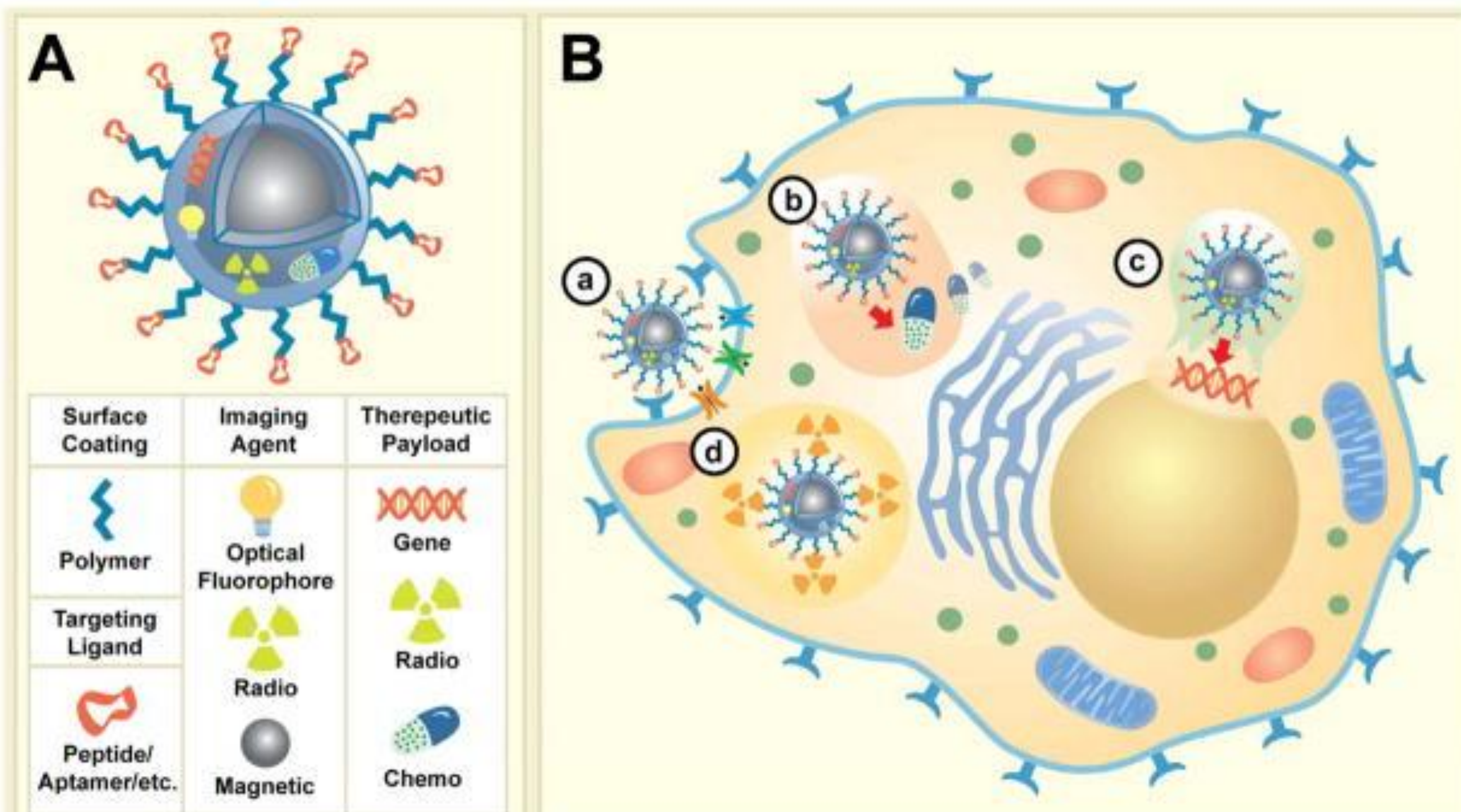

Illustration of multifunctional imaging/therapeutic MNPs anatomy and potential mechanisms of action at the cellular level. (A) A multifunctional MNP modified with targeting ligands extended from MNP surface with polymeric extenders, imaging reporters (optical, radio, magnetic), and potential therapeutic payloads (gene, radio, chemo). (B) Four possible modes of action for various therapeutic agents; a) Specific MNP binding to cell surface receptors (i.e. enzymes/proteins) facilitate their internalization and/or inactivation, b) controlled intercellular release of chemotherapeutics; c) release of gene therapeutic materials post endosomal escape and subsequent targeting of nucleus; and d) intracellular decay of radioactive materials.

Omid Veiseh at al. Adv Drug Deliv Rev. 2010 March 8; 62(3): 284–304.

III. Cellular studies and potential biomedical application for pathological cell detection, tagging and treatment.

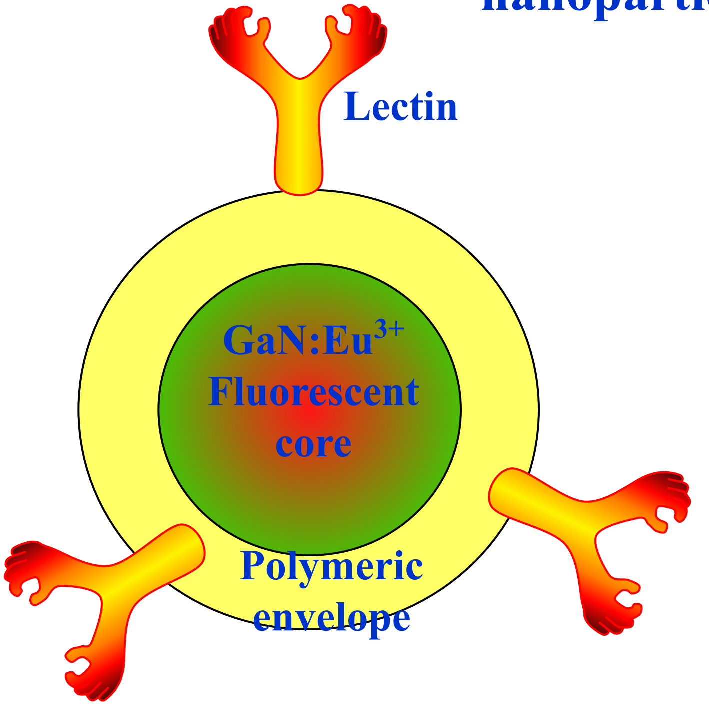

$GaN:Eu^{3+}$-PSL lectin conjugated nanoparticles

SEM image for pure GaN nanoparticles

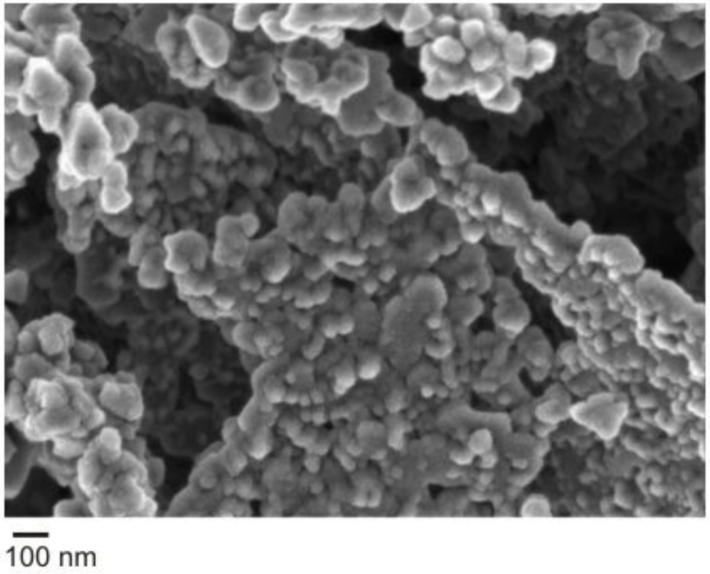

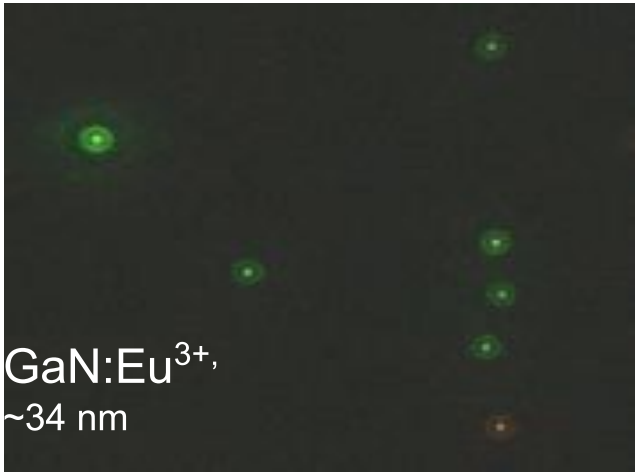

Fluorescence of $GaN:Eu^{3+}$ nanoparticles

III. Cellular studies and potential biomedical application for pathological cell detection, tagging and treatment.

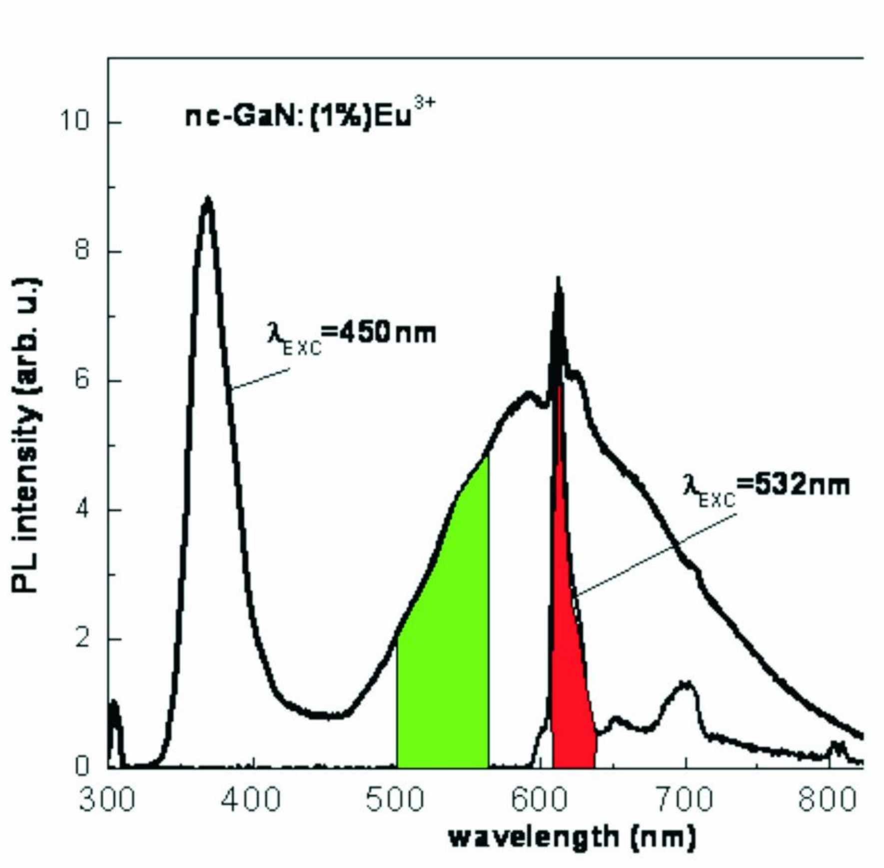

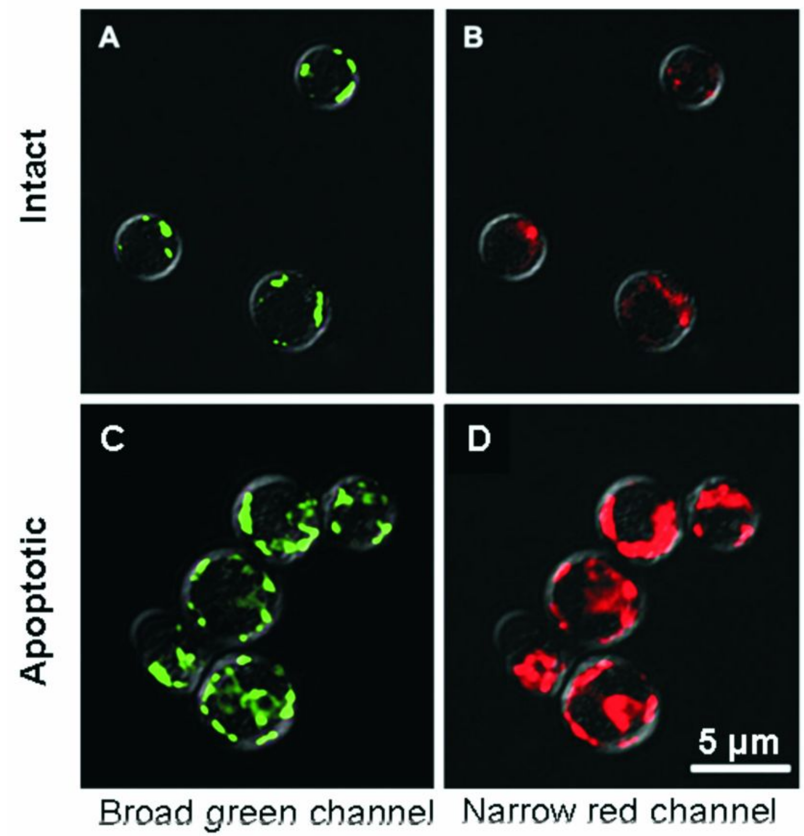

Bioconjugated nanoparticles GaN:Eu3+-PSL lectin specifically bind to apoptotic cells

III. Cellular studies and potential biomedical application for pathological cell detection, tagging and treatment.

Labeling dying cell by fluorescein-encapsulated functional nanoparticles

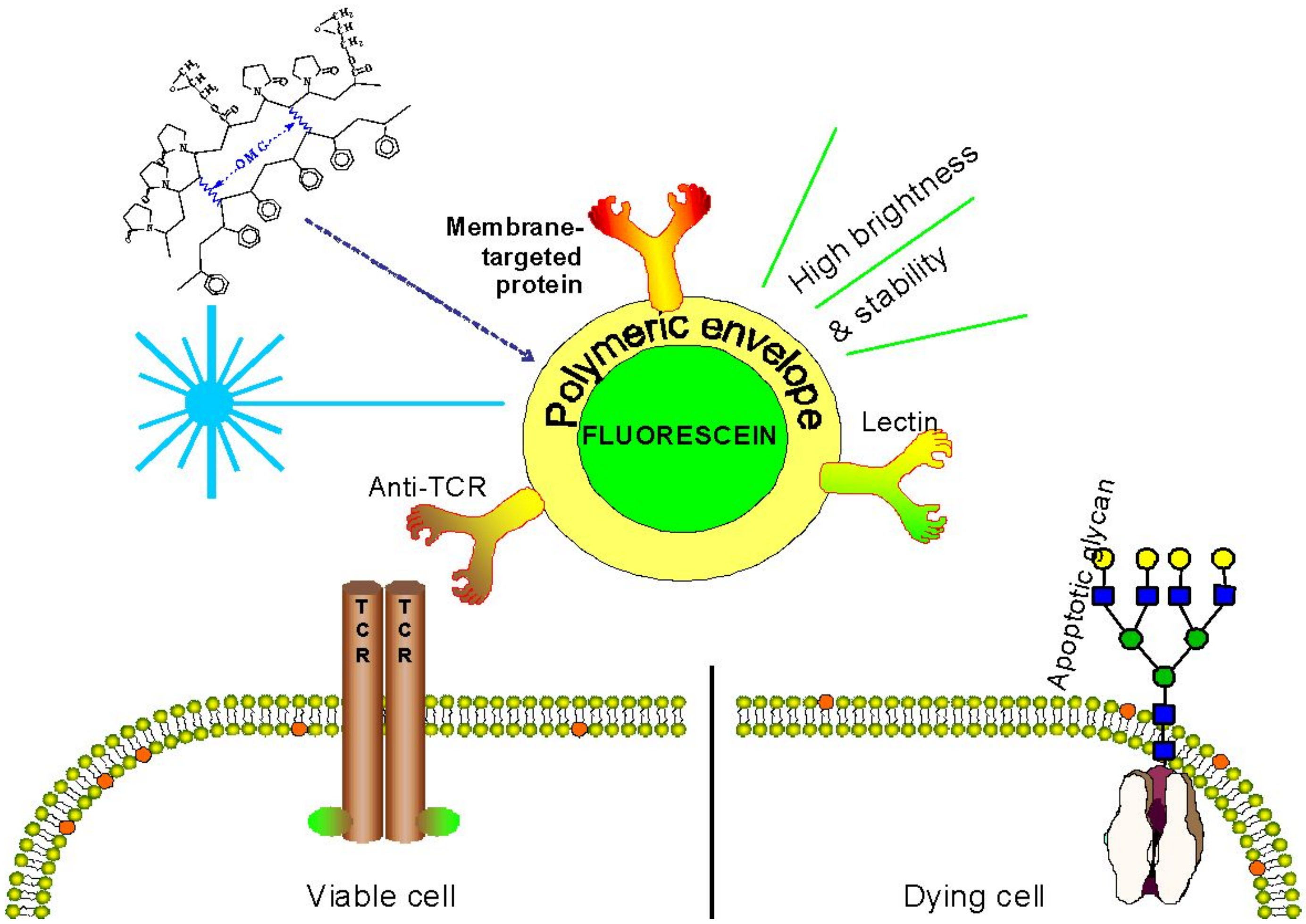

III. Cellular studies and potential biomedical application for pathological cell detection, tagging and treatment.

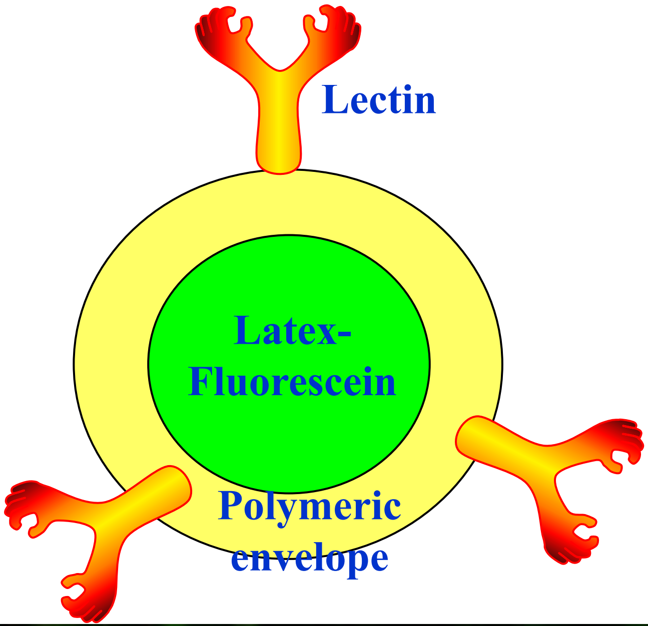

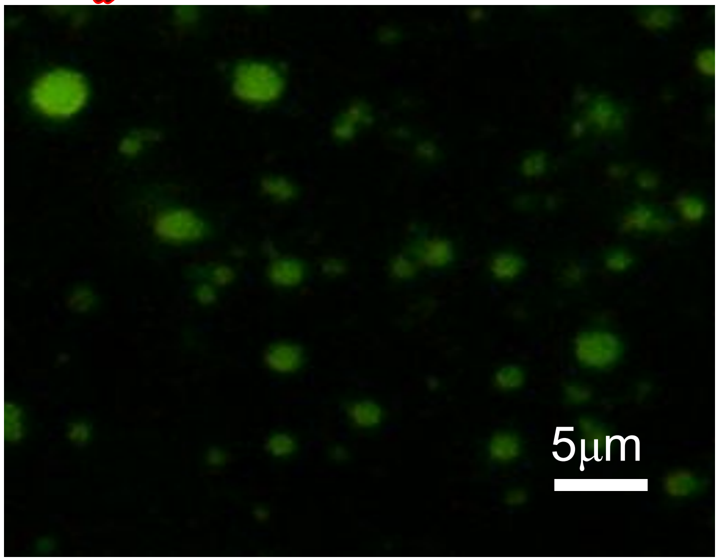

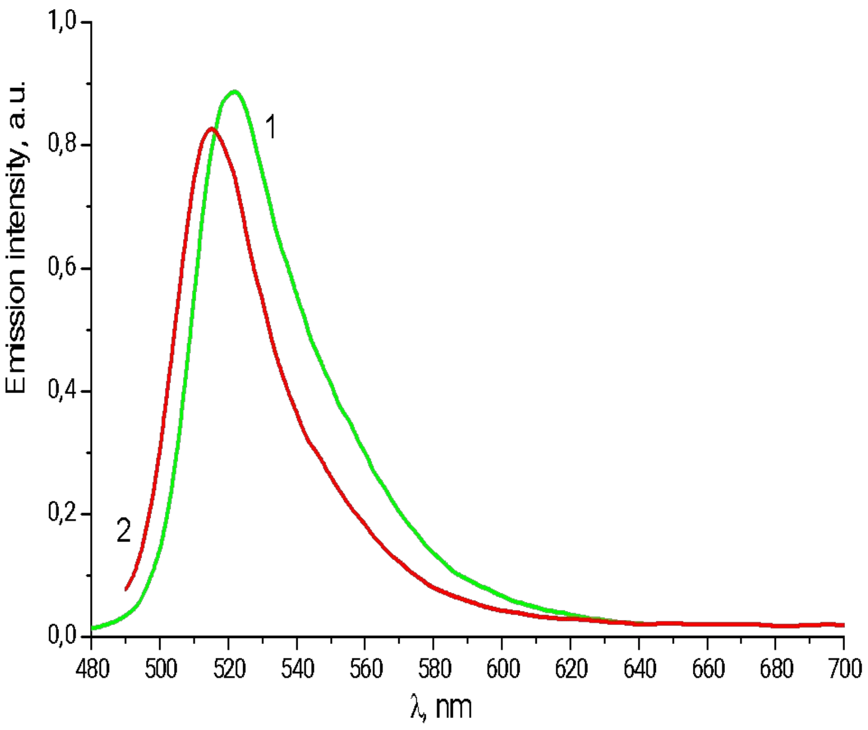

Emission spectra of fluorescein (1) and fluorescein-containing latex nanoparticles (2); excitation at 425 nm.

III. Cellular studies and potential biomedical application for pathological cell detection, tagging and treatment.

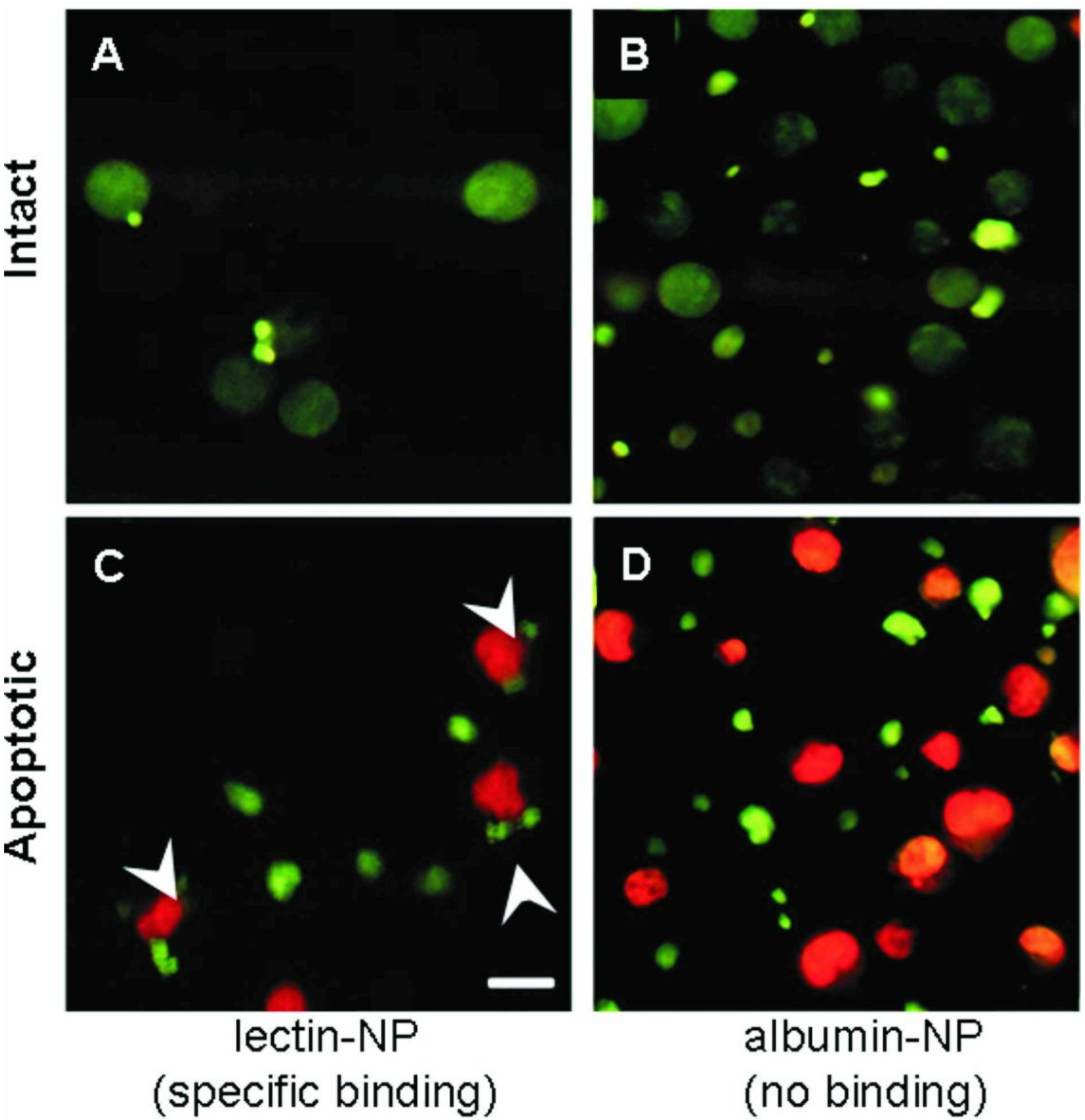

Bioconjugated fluorescein-containing WGA-lectin-conjugated nanoparticles used for the detection of necrotic cells

In A and B living cells are counterstained with 1:100,000 (w/v) acridine orange solution (fain green), in C and D dead cells are counterstained with propidium iodine (1 |jg/ml) solution to visualize nuclei of dead cells (red). White bar correspond to 5 µm

III. Cellular studies and potential biomedical application for pathological cell detection, tagging and treatment.

Targeted biodegradation of polymeric nanoconjugates

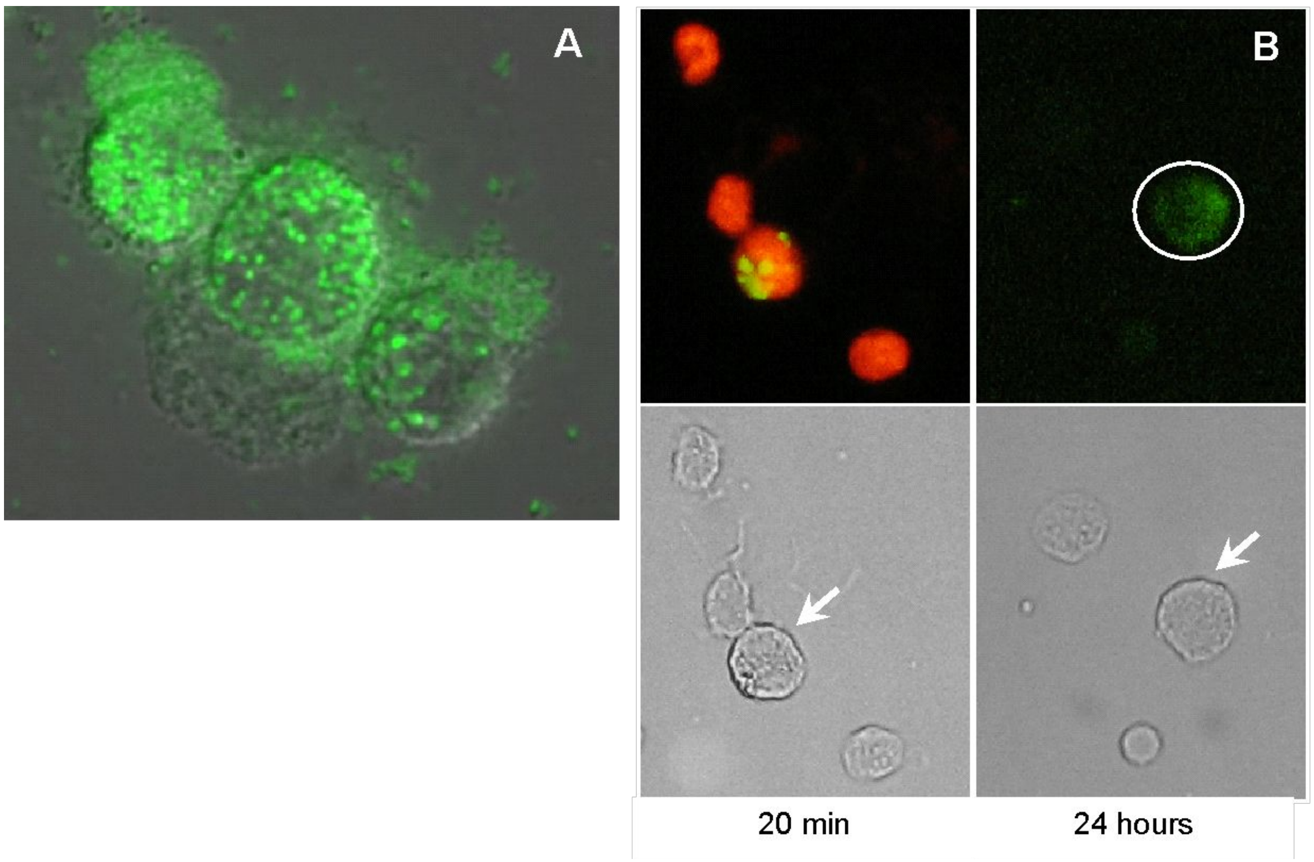

A - BSA-conjugated fluorescein-containing nanoparticles (~200 nm) are bound to murine macrophages of J774.2 line after 20 min incubation. DIC with superimposed fluorescent image. B – Ig-conjugates fluorescein-containing nanoparticles (~300 nm) were injected into the peritoneal cavity of mice. After 20 min and 24 h, peritoneal cells were removed, washed, concentrated and studied. Top panel – fluorescent microscopy; lower panel – light microscopy. Macrophages (indicated by arrow) were identified on the basis of their morphology and propidium iodine (20 min, red color) or DAPI counterstaining (not shown). Note that after 24 h NPs were digested by the macrophages

III. Cellular studies and potential biomedical application for pathological cell detection, tagging and treatment.

a b

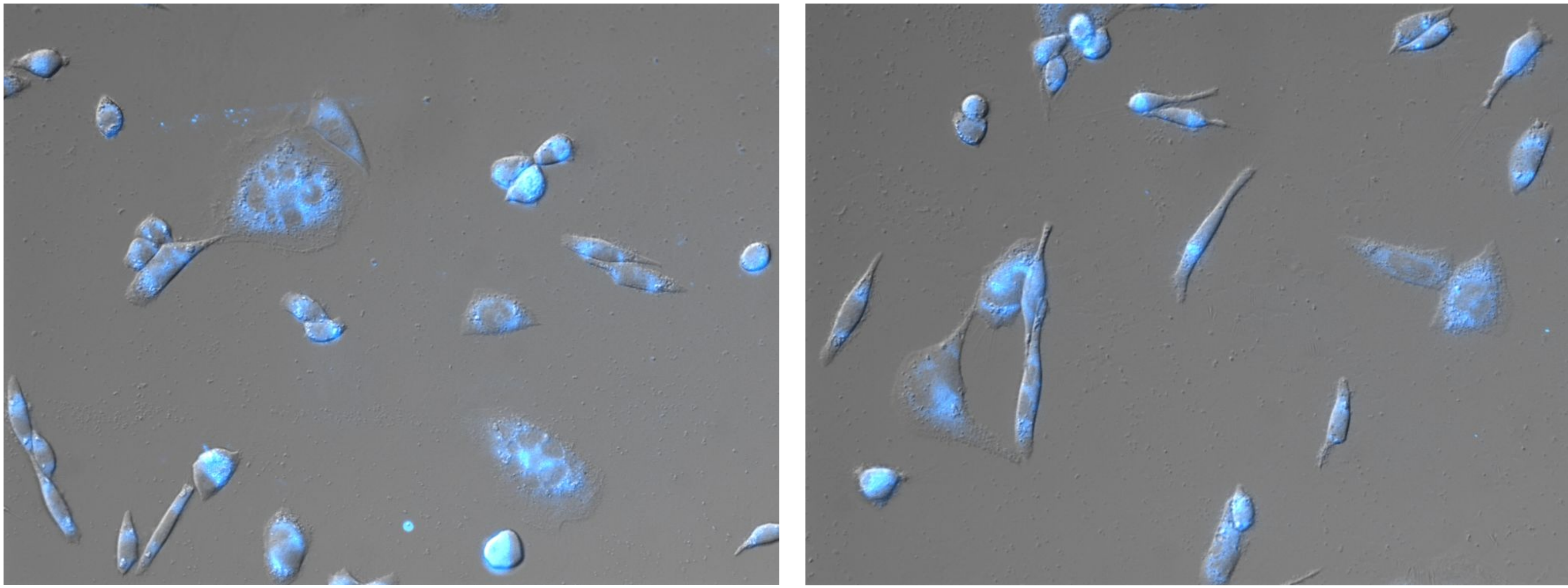

Engulfment of pyrazolyn-containing functional polymeric nanoparticles by melanoma cells; concentration of nanparticles in water dispersion – 0.1%, a) 1 microliter per 1 ml of cultural medium; b) 10 microliter per 1 ml of cultural medium (incubation 24h)

III. Cellular studies and potential biomedical application for pathological cell detection, tagging and treatment.

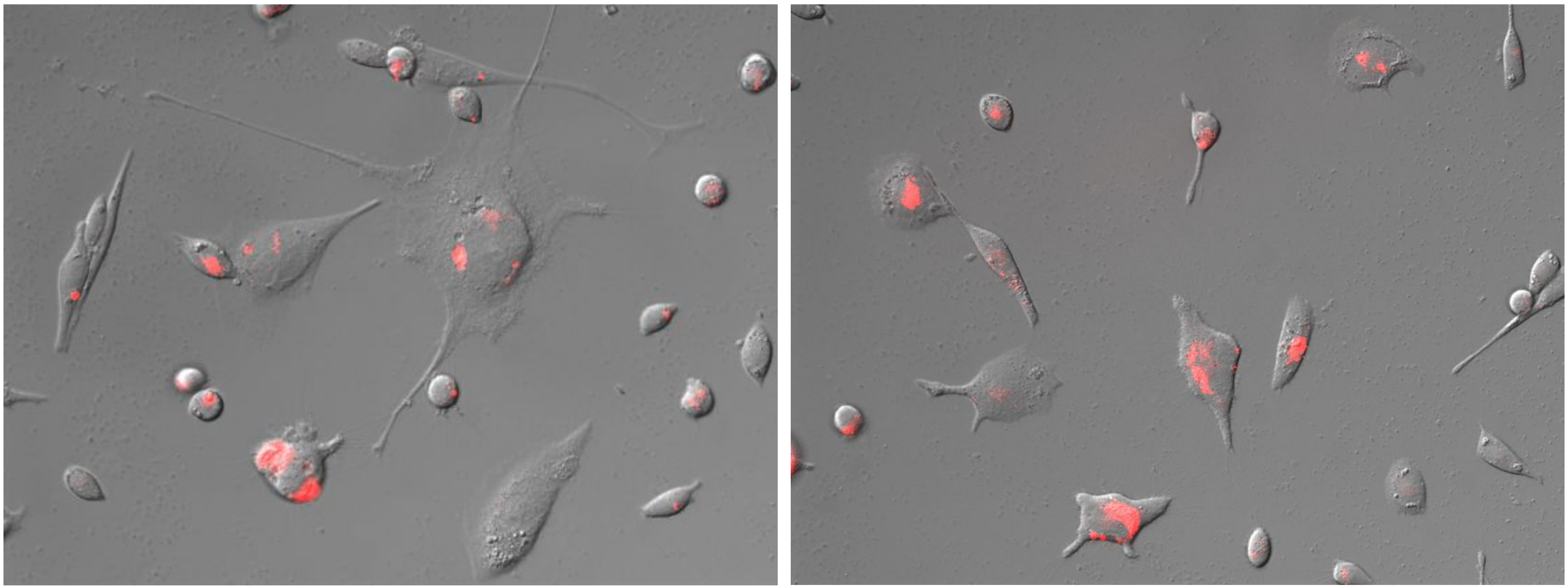

a b

Engulfment of functional oligoelectrolyte based nanogels filled with complex Eu(TTA)$_3$ TFFO by melanoma cells; concentration of nanogels in water dispersion – 0.1%, a) 1 microliter per 1 ml of cultural medium; b) 10 microliter per 1 ml of cultural medium (incubation 24h)

III. Cellular studies and potential biomedical application for pathological cell detection, tagging and treatment.

Potential using functional nanoscintillators for radiotherapy of tumors

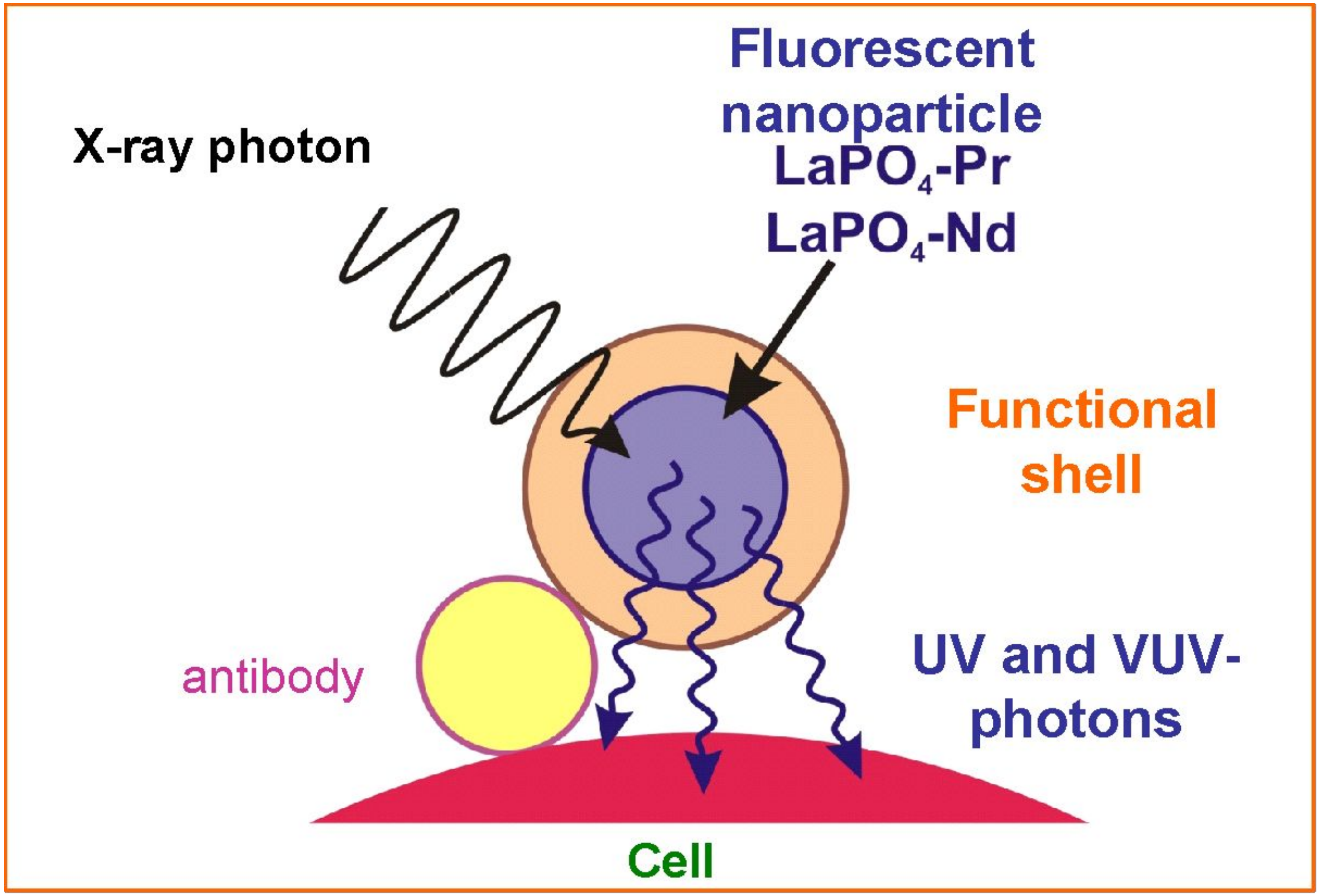

III. Cellular studies and potential biomedical application for pathological cell detection, tagging and treatment.

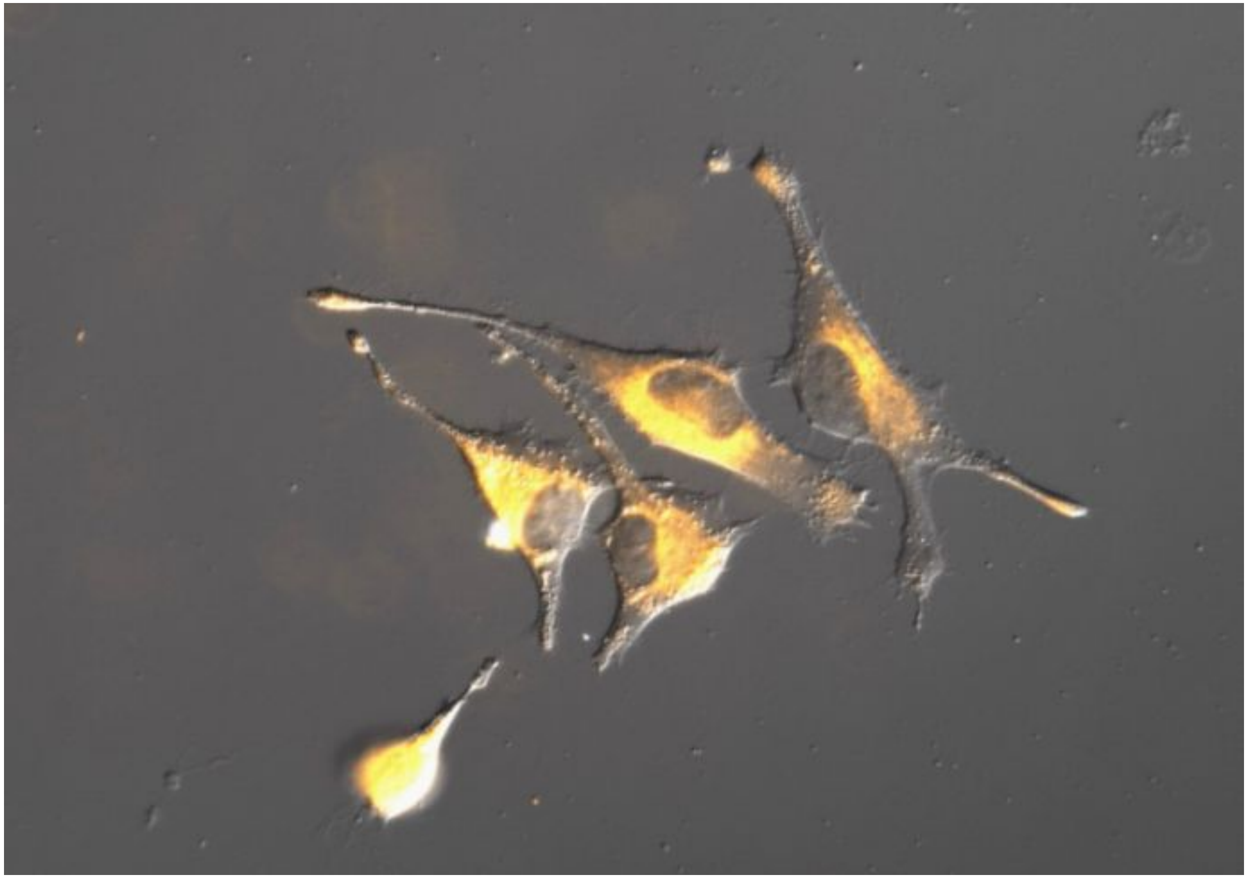

Engulfment of functional nanosized scintillators based on $LaPO_4$…Pr by human melanoma cells line SK-MEL-28.

Acknowledgements

Many thanks to my team and partners

Dr. N. Mitina, Dr. O. Hevus, Dr. O. Shapoval, PhD students O. Myagkota from Lviv Polytechnic National University;

Professor A. Voloshinovskii, Professor A. Gektin, Dr. P. Zhmurin, Dr. V. Vistovskiy from I. Franko National University and Kharkiv Institute of Scintillation Materials of NASU

- **Professor R. Stoika, Dr. R. Bilyy, Dr. R. Panchuk and team from Cell Biology Institute of NASU**

for the experimental work as well as for the collaboration, ideas and discussion

 70